

AD \_\_\_\_\_

Award Number: DAMD17-99-1-9333

TITLE: A Structure Based, Solid Phase Synthesis Approach to the Development of Novel Selective Estrogen Receptor Modulatory Steroids

PRINCIPAL INVESTIGATOR: Robert N. Hanson, Ph.D.

CONTRACTING ORGANIZATION: Northeastern University  
Boston, Massachusetts 02115

REPORT DATE: July 2001

TYPE OF REPORT: Annual

PREPARED FOR: U.S. Army Medical Research and Materiel Command  
Fort Detrick, Maryland 21702-5012

DISTRIBUTION STATEMENT: Approved for Public Release;  
Distribution Unlimited

The views, opinions and/or findings contained in this report are those of the author(s) and should not be construed as an official Department of the Army position, policy or decision unless so designated by other documentation.

20020717 052

# REPORT DOCUMENTATION PAGE

Form Approved  
OMB No. 074-0188

Public reporting burden for this collection of information is estimated to average 1 hour per response, including the time for reviewing instructions, searching existing data sources, gathering and maintaining the data needed, and completing and reviewing this collection of information. Send comments regarding this burden estimate or any other aspect of this collection of information, including suggestions for reducing this burden to Washington Headquarters Services, Directorate for Information Operations and Reports, 1215 Jefferson Davis Highway, Suite 1204, Arlington, VA 22202-4302, and to the Office of Management and Budget, Paperwork Reduction Project (0704-0188), Washington, DC 20503

1. AGENCY USE ONLY (Leave blank)	2. REPORT DATE	3. REPORT TYPE AND DATES COVERED	
	July 2001	Annual (1 Jun 00 - 31 May 01)	
4. TITLE AND SUBTITLE A Structure Based, Solid Phase Synthesis Approach to the Development of Novel Selective Estrogen Receptor Modulatory Steroids			5. FUNDING NUMBERS DAMD17-99-1-9333
6. AUTHOR(S) Robert N. Hanson, Ph.D.			
7. PERFORMING ORGANIZATION NAME(S) AND ADDRESS(ES) Northeastern University Boston, Massachusetts 02115  E-Mail: r.hanson@neu.edu			8. PERFORMING ORGANIZATION REPORT NUMBER
9. SPONSORING / MONITORING AGENCY NAME(S) AND ADDRESS(ES) U.S. Army Medical Research and Materiel Command Fort Detrick, Maryland 21702-5012			10. SPONSORING / MONITORING AGENCY REPORT NUMBER
11. SUPPLEMENTARY NOTES			
12a. DISTRIBUTION / AVAILABILITY STATEMENT Approved for Public Release; Distribution Unlimited			12b. DISTRIBUTION CODE
13. ABSTRACT (Maximum 200 Words) The objective of this project is the development of new chemotherapeutic agents for the treatment of hormone-responsive breast cancer using a structure-based solid phase synthesis approach. During the past year we have utilized our functionalized resin to prepare a second series of carboxamido-phenylvinyl estradiols. The compounds were characterized by NMR and analyzed by computational methods. The new agents were evaluated for estrogen receptor binding affinity and in vivo efficacy. The results suggest that incorporation of functional groups at the specific sites proposed reduces both affinity and efficacy, however, positional isomers and configurational isomers had better activity. These observations have been incorporated into the design of the second generation steroids that will be prepared and evaluated in the third year of the project.			
14. SUBJECT TERMS Breast Cancer			15. NUMBER OF PAGES 72
			16. PRICE CODE
17. SECURITY CLASSIFICATION OF REPORT Unclassified	18. SECURITY CLASSIFICATION OF THIS PAGE Unclassified	19. SECURITY CLASSIFICATION OF ABSTRACT Unclassified	20. LIMITATION OF ABSTRACT Unlimited

FOREWORD

Opinions, interpretations, conclusions and recommendations are those of the author and are not necessarily endorsed by the U.S. Army.

 Where copyrighted material is quoted, permission has been obtained to use such material.

       Where material from documents designated for limited distribution is quoted, permission has been obtained to use the material.

       Citations of commercial organizations and trade names in this report do not constitute an official Department of Army endorsement or approval of the products or services of these organizations.

N/A In conducting research using animals, the investigator(s) adhered to the "Guide for the Care and Use of Laboratory Animals," prepared by the Committee on Care and use of Laboratory Animals of the Institute of Laboratory Resources, national Research Council (NIH Publication No. 86-23, Revised 1985).

N/A For the protection of human subjects, the investigator(s) adhered to policies of applicable Federal Law 45 CFR 46.

N/A In conducting research utilizing recombinant DNA technology, the investigator(s) adhered to current guidelines promulgated by the National Institutes of Health.

N/A In the conduct of research utilizing recombinant DNA, the investigator(s) adhered to the NIH Guidelines for Research Involving Recombinant DNA Molecules.

N/A In the conduct of research involving hazardous organisms, the investigator(s) adhered to the CDC-NIH Guide for Biosafety in Microbiological and Biomedical Laboratories.

  
FI - Signature

11 / 30 / 01  
Date

## Table of Contents

1. Cover	1
2. SF 298	2
3. Foreword	3
4. Table of Contents	4
5. Introduction	5
6. Body	6-12
7. Key Research Accomplishments	12
8. Reportable Outcomes	13
9. Conclusions	14
10. References	14
11. Appendix	14

## **5. Introduction**

The overall objective of this project is the development of new chemotherapeutic agents for the treatment of hormone-responsive breast cancer. Based upon our precious synthetic work and molecular modeling studies, we undertook the preparation of a series of  $17\alpha$ -(substituted phenylvinyl) estradiols using a solid-phase synthesis approach. This would be accompanied by the development of the appropriate biological assays and NMR evaluations. The preliminary aspects of this work were described in the first progress report. In this report we describe the advances that we have made in these areas.

## **6. Body**

The research proposal described 5 Tasks as part of the Statement of Work. These included: 1. Synthesis of polymer-bound aminomethyl- and carboxy-phenylvinyl estradiol, 2. Synthesis, isolation and purification of structure-based libraries, 3. Determination of biological properties, 4. Assessment of structure-activity relationships, and 5. Synthesis, purification, characterization and evaluation of a second library of compounds. Work has been undertaken on the first four tasks and will be described in the report.

### **Task 1. Synthesis of polymer bound $17\alpha$ -(3-aminomethylphenyl) and $17\alpha$ -(4-carboxyphenyl)vinyl estradiol.**

During the past year we have prepared the polymer bound  $17\alpha$ -(4-carboxyphenyl)vinyl estradiol as proposed. The procedure involved the synthesis of 2-trimethylsilyl ethyl 4-iodobenzoate which was coupled to the polymer bound  $17\alpha$ -tributylstannylvinyl estradiol using the Stille reaction conditions. The trimethylsilyl ethyl protecting group was easily removed with tetrabutyl ammonium fluoride in THF. The resultant product could then be activated using usual carboxy reagents for preparation of target compounds. The overall yields to this point were good (70%) based on cleavage of the carboxyphenylvinyl estradiol from the resin using methoxide in methanol. It should

be noted that the work so far focused on the E-(X-phenyl)vinyl estradiols and that modifications would be necessary to extend the methodology to the corresponding Z-isomers as discussed in subsequent sections of the report.

**Task 2. Synthesis, Isolation, Purification and Characterization of the Directed Libraries**

Using the polymer bound  $17\alpha$ -(4-carboxyphenyl)vinyl estradiol described in Task 1, we have prepared a series of amide derivatives. This included the N-methyl, N-benzyl, N-(2-phenylacetic methyl ester) and the N,N-dimethyl compounds. One Z-isomer was isolated as a minor product from the reactions that were performed on a .2mmole scale. The isolated yields for this process were low (<40%) and need to be improved.

Additional polymer bound tributylstannylvinyl estradiol (E-isomer) has been prepared to explore alternatives to this approach. This alternative approach involves the synthesis of the (2/3/4)- iodobenzylamines substituted with the appropriate acyl(aminoacyl) group or the (2/3/4)-iodobenzoyl groups substituted with the appropriate amine (carboxyamine) group. We have begun to generate these intermediates. The typical yields so far have been 70-80% (isolated). The advantage at this point is that these intermediates are readily accessible and can be used in one step with the solid phase reagent to give the product. In addition, we can extend their use to the corresponding Z-isomers with either solution or solid phase chemistry.

We have undertaken conformational analyses of the steroids using NMR and molecular modeling. So far we have evaluated the E- and Z- mono-substituted

phenylvinyl estradiols that were prepared in earlier studies. These results are described in two publications by Sebag, et al. (Appendix) Molecular modeling and NMR studies suggest that the rotational barrier around the vinyl phenyl bound is low for the meta and para isomers and therefore several low energy conformers may be accessible at the ligand binding site. Substitution at the ortho position introduces rotational barriers that restrict the conformations of the ligands. This effect will be discussed in the section on structure-activity relationships.

Another aspect that is being considered is the use of vinyl boronic acids as the estradiol coupling unit and preliminary work has begun to examine that chemistry. The synthesis of model arylvinyl boronic acids and their coupling to representative aryl iodides has been accomplished and can be applied to the synthesis of target compounds, if necessary.

### **Task 3. Measurement of Biological Properties.**

During this phase of the project we have continued the evaluation of the target compounds as ligands for the estrogen receptor. Using the conditions established in the first year, we have completed the competitive binding assays for the first series of 4-carboxy amides in the E-isomers as well as one of the Z-isomers. The methylamido-, benzylamido and phenylglycylamido compounds had RBA values in the 1-4 range, significantly lower than the parent unsubstituted phenylvinyl estradiol (RBA = 9-16) and lower than the analogous methyl ester (RBA = 15-26). The RBA value for the E-benzamido-product was also significantly less than that for corresponding Z-benzamido-

product (4 vs. 10-26). Measurement of newer compounds will be enhanced by the recent purchase 96-well plate reader that is more rapid and efficient than the previous instrument. This will be particularly valuable in the next year as we complete the synthesis of several series of compounds.

We have continued to develop the methodology for the MCF-7 cell proliferation assay. The addition of the aforementioned plate reader is most applicable to this assay. Re-evaluation of compounds using this instrument and improving the assay conditions has resulted in a reinterpretation of previous results. Some of the ligands that appeared to be antagonists are more correctly weak agonists, showing proliferative properties at higher doses. Therefore, further developmental work on this assay continues.

While the in vitro assay work is being improved, we have proceeded to initial in vivo uterotrophic growth assays to evaluate efficacy. One of the major difficulties with this assays involved the inconsistencies in animal weights, variation in lots from the supplier. Results from one assay could not be directly compared to a subsequent assay. As a result, we have undertaken evaluating an entire series of compounds ( e.g., ortho-, meta-, para-, E- and Z-isomers, plus standards) with a single large lot of immature female rats (> 250 animals). This method gives internal consistency, particularly to establish orders of potency and efficacy. For this project we have evaluated the entire series of methyl esters which had been prepared as part of another bio-organic project. This experiment, while time consuming, has provided valuable insights into our (anti)estrogenic drug design program.

#### **Task 4. Assessment of Structure-Activity Relationships.**

During the past year we have generated enough data to begin the process of structure-activity relationships (SAR). For this report, we will look specifically at the two series that we have prepared and evaluated as part of this project plus the set of methyl esters prepared as part of another project. For the meta-aminomethyl compound and the acylated derivatives, the parent meta-aminomethyl compound had the best receptor binding properties, with all of the acylated compounds having RBA values an order of magnitude lower (18-19 vs. 1-5). The size of the acyl group did not have any clear effect since acetyl-, benzoyl- and t-Boc groups had similar values. Interestingly, the values were similar to those observed for the meta-carboxylic acid (RBA= 1-2) suggesting that perhaps electronic rather than steric effects are involved. Molecular modeling studies are in progress to help elucidate these observations. For the para-carboxamides, amido substitution also appears to be detrimental to binding in the E-isomeric series. The methyl-, benzyl- and phenylglycylamido- products were all weaker ligands than the corresponding methyl ester (RBA =1-4 vs. 15-26). As in the meta-series, these values are similar to the para-carboxylic acid (RBA= 1-2). However, the Z-benzylamido analog was reasonably potent with an RBA value = 10-26. The results from these two series suggest that, at least for receptor affinity, the substitutions at the meta-aminomethyl and para-carboxamido- positions are detrimental. The Z-isomers at these positions certainly appear

to have higher affinity and may tolerate more elaborate substituents. As a result, our design of subsequent series of compounds must take these observations into consideration.

The results of the initial in vivo uterotrophic growth assay in immature female rats was conducted with the full series of carboxymethyl-phenylvinyl estradiol isomers (6 compounds. In this study, all of the compounds were agonists and elicited responses equal to estradiol at their highest dose. Several trends were noted in this initial study. First, there was a poor correlation between the RBA value and the dose that equaled 50% of the 10 n mole estradiol dose. While RBA values for this series varied from 6/12 for the E-meta isomer up to 72/57 for the Z-para, the 50% dose varied from 0.25 n moles (Z-para) to > 3000 n moles (E-para). Also, the rank order of potency was different between the two assays. For ER-LBD binding the order was Z-para->Z-ortho-=E-ortho->E-meta-=E-para->Z-meta-, and the potency order was Z-para-> Z-ortho-=E-ortho->Z-meta->E-meta-> E-para-. Since these compounds were run simultaneously, the results have major implications for this project. The E-meta- and E-para- compounds that formed the basis for the synthetic approach express the weakest in vivo effects, at least as agonists. If this response correlates with an inhibition of proliferative effects, these compounds continue to have therapeutic potential. Should these compounds only be weak in vivo agonists, then attention should shift to the preparation and evaluation of modified E-ortho- or Z-ortho-/para derivatives. Further biological studies coupled with our ongoing NMR and

molecular modeling work may provide keys into the structural factors that determine estrogen receptor affinity and/or efficacy.

**Task 5. Synthesis, Purification, Characterization and Evaluation of a Second Library of Compounds.**

This portion of the project has just been started. Based upon the initial biological results obtained during this past year, we have modified the target compounds for the second generation. Two modifications that we will be exploring involve the preparation of ortho- and meta-substituted amides and the corresponding Z-isomers. Some process development will be involved as we go from the E- to Z- compounds, but we have done solution chemistry on similar agents.

**7. Key Accomplishments.**

- Preparation of the 4-carboxamide and 3-acylaminomethyl derivatives of E-phenylvinyl estradiol
- Completed NMR studies of E- and Z-substituted phenylvinyl estradiols
- Binding studies with ER-LBD indicated decreased affinity of substituted carboxamides and acylaminomethyl derivatives compared to ester or unsubstituted compounds
- Uterotrophic assays indicate a disconnect between in vitro affinity and in vivo potency, with Z-isomers and the E-ortho compounds being most potent
- Structure-activity relationship studies suggest expanding the synthetic targets to include Z-isomers of the aminoacyl derivatives of the phenylvinyl estradiol

## **8. Reportable Outcomes.**

- a. Manuscripts, abstracts, presentations
  1. Sebag, A.B., Friel, C. J., hanson, R.N., and Forsyth, D. A. Conformational studies on (17 $\alpha$ ,20Z)-21-(X-phenyl)-19-norpregna-1,3,5(10),20-tetraene-3,17 $\beta$ -diols using 1D and 2D NMR spectroscopy and GIAO calculations of C-13 shieldings. *J. Org. Chem.* (2000) 65, 7902-7912.
  2. Hanson, R.N. Synthesis of Auger electron-emitting radiopharmaceuticals. *Curr. Pharm. Design* (2000) 6, 1457-1468.
  3. Sebag, A.B., Hanson, R.N., Forsyth, D.A., and Lee, C.-Y., Conformational studies of novel estrogen receptor ligands by 1D and 2D NMR spectroscopy and computational methods. *Org. Magn. Res.* (accepted pending minor revisions).
  4. Hanson, R.N., Design, synthesis and evaluation of novel steroidal antiestrogens for the treatment of hormone responsive breast cancer. Invited presentation at The Philip S. Portoghese Symposium in Medicinal Chemistry, August 23-24, 2001, Minneapolis, Minnesota.

## **9. Conclusions.**

At this point we have achieved several intermediate objectives of the project. We have demonstrated the feasibility of the functionalized resin as a method for preparing the target steroidal derivatives. We have developed the methods for rapidly screening the new compounds for their receptor affinity using the ER-LBD, and for extending this to the MCF-7 and in vivo uterotrophic assays. We have generated preliminary SARs for our initial series of compounds and found that other structural isomers may have better properties than those identified in the proposal. These observations will be incorporated into the second generation of compounds that will be prepared and evaluated in the third year of the project. Several manuscripts are in preparation to report on these results.

## **10. References.**

None.

## **11. Appendix.**

The appendix material is comprised of three copies of the two published manuscripts, the accepted manuscript and the bulletin for the Symposium.

---

**Conformational Studies on (17 $\alpha$ ,20 $Z$ )-21-(*X*-Phenyl)-19-norpregna-1,3,5(10),  
20-tetraene-3,17 $\beta$ -diols Using 1D and  
2D NMR Spectroscopy and GIAO  
Calculations of  $^{13}\text{C}$  Shieldings**

---

**Albert B. Sebag, Carolyn J. Friel, Robert N. Hanson, and  
David A. Forsyth**

Departments of Pharmaceutical Science and Chemistry, Northeastern  
University, 360 Huntington Avenue, Boston, Massachusetts 02115

**The Journal of  
Organic  
Chemistry®**

Reprinted from  
Volume 65, Number 23, Pages 7902–7912

# Conformational Studies on (17 $\alpha$ ,20Z)-21-(X-Phenyl)-19-norpregna-1,3,5(10),20-tetraene-3,17 $\beta$ -diols Using 1D and 2D NMR Spectroscopy and GIAO Calculations of $^{13}\text{C}$ Shieldings

Albert B. Sebag, Carolyn J. Friel, Robert N. Hanson,\* and David A. Forsyth

*Departments of Pharmaceutical Science and Chemistry, Northeastern University, 360 Huntington Avenue, Boston, Massachusetts 02115*

*r.hanson@nunet.neu.edu*

*Received May 24, 2000*

Differences in agonist responses of the novel estrogen receptor ligands (17 $\alpha$ ,20Z)-(p-methoxyphenyl)-vinyl estradiol (**1**), (17 $\alpha$ ,20Z)-(o- $\alpha$ , $\alpha$ , $\alpha$ -trifluoromethylphenyl)vinyl estradiol (**2**), and (17 $\alpha$ ,20Z)-(o-hydroxymethylphenyl)vinyl estradiol (**3**) led us to investigate their solution conformation. In competitive binding assay studies, we observed that several phenyl-substituted (17 $\alpha$ ,20E/Z)-(X-phenyl)vinyl estradiols exhibited significant estrogen receptor binding, but with variation (RBA (**1**) = 20; RBA (**2**) = 23; RBA (**3**) = 140 where estradiol RBA = 100) depending on the phenyl substitution pattern. Because the 17 $\alpha$ -phenylvinyl substituent interacts with the key helix-12 of the ligand binding domain, we considered that differences in the preferred conformation of **1–3** could account for their varying binding affinity. 2D NMR experiments at 500 MHz allowed the complete assignment of the  $^{13}\text{C}$  and  $^1\text{H}$  spectra of **1–3**. The conformations of these compounds in solution were established by 2D and 1D NOESY spectroscopy. A statistical approach of evaluating contributing conformers of **1–3** from predicted  $^{13}\text{C}$  shifts correlated quite well with the NOE data. The 17 $\alpha$  substituents of **1** and **2** exist in similar conformational equilibria with some differences in relative populations of conformers. In contrast, the 17 $\alpha$  substituent of **3** exists in a different conformational equilibrium. The similarity in solution conformations of **1** and **2** suggests they occupy a similar receptor volume, consistent with similar RBA values of 20 and 23. Conversely, the different conformational equilibria of **3** may contribute to the significant binding affinity (RBA = 140) of this ligand.

## Introduction

Breast cancer is the most common form of cancer among women in the United States, with approximately 181 000 new cases diagnosed annually.<sup>1</sup> It is estimated that one in eight women will develop breast cancer during their lifetime and one in three of those will die from the disease. Among the newly diagnosed cases, about 60% are classified as hormone responsive, defined as containing a minimal level of estrogen receptor (ER) and requiring the presence of circulating estrogen to maintain tumor growth.<sup>2</sup> As part of our program to develop more effective therapeutic agents for the treatment of breast cancer, we undertook the design of new compounds that can potently and selectively block the interaction of estradiol with its target receptor.

Our synthetic efforts have focused on the 17 $\alpha$  position of estrogen as the site for introducing substituents that would impart the desired biological properties. Unlike previous studies with 17 $\alpha$  alkyl, aryl, or alkynyl groups, suggesting that substituents larger than propyl or propynyl were poorly tolerated,<sup>3</sup> we found that the 17 $\alpha$

X-vinyl estradiols could bind quite well to the estrogen receptor.<sup>4</sup> Even large substituents, where X = C<sub>6</sub>H<sub>5</sub>, SeC<sub>6</sub>H<sub>5</sub>, or SC<sub>6</sub>H<sub>5</sub>, exhibited significant relative binding affinities (RBA) for the receptor.<sup>5</sup> These observations led us to pursue the synthesis and evaluation of (17 $\alpha$ ,20Z)-21-(X-phenyl)-19-norpregna-1,3,5(10),20-tetraene-3,17 $\beta$ -diols (referred to herein as phenylvinyl estradiols) as probes for the estrogen receptor, the results of which are reported in detail elsewhere.<sup>6</sup>

We observed that several phenyl-substituted (17 $\alpha$ ,20E/Z)-(X-phenyl)vinyl estradiols exhibited significant estrogen receptor binding (RBA  $\geq$  20 where estradiol RBA = 100 at 2 °C), but with variation depending on the phenyl substitution pattern (Figure 1). (17 $\alpha$ ,20Z)-(p-Methoxyphenyl)vinyl estradiol (**1**), for example, exhibited modest agonist responses in vitro and in vivo and shows an RBA of 20 in vitro, while (17 $\alpha$ ,20Z)-(o- $\alpha$ , $\alpha$ , $\alpha$ -trifluoromethylphenyl)vinyl estradiol (**2**) was similarly potent with an

(1) Greenlee, R. T.; Murray, T.; Bolden, S.; Wingo, P. A. *Cancer J. Clin.* **2000**, *4*, 33.

(2) Iacobelli, S.; King, R. J. B.; Lidner, H. R.; Lippman, M. E. In *Hormones and Cancer*; Raven Press: New York, 1980; Vol. 15, p 337.

(3) (a) Counsell, R. E.; Klimstra, P. D.; Elton, R. L.; Nutting, E. E. *J. Med. Chem.* **1968**, *9*, 689. (b) Raynaud, J. P.; Ojasoo, T. *J. Steroid Biochem.* **1986**, *25*, 811. (c) Salman, M.; Reddy, B. R.; Ray, S.; Stotter, P. L.; Chamness, G. C. *J. Steroid Biochem.* **1988**, *30*, 539.

(4) (a) Hanson, R. N.; El-Wakil, H. *J. Org. Chem.* **1987**, *52*, 3687. (b) Napolitano, E.; Fiaschi, R.; Hanson, R. N. *J. Med. Chem.* **1991**, *34*, 2754. (c) Hanson, R. N.; Napolitano, E.; Fiaschi, R. *J. Med. Chem.* **1998**, *41*, 4686.

(5) (a) Napolitano, E.; Fiaschi, R.; Herman, L. W.; Hanson, R. N. *Steroids* **1996**, *61*, 384. (b) Herman, L. W.; Fiaschi, R.; Napolitano, E. *Steroids* **1996**, *61*, 718. (c) Hanson, R. N.; Napolitano, E.; Fiaschi, R. *Steroids* **1998**, *63*, 479.

(6) (a) Lee, C. Y.; Hanson, R. N., in press. (b) Hanson, R. N.; Lee, C. Y.; Friel, C. *J. Med. Chem.*, submitted for publication. (c) Hanson, R. N.; Friel, C.; Deth, R. C.; DeSombre, E. R.; Metaghee, A. *J. Med. Chem.*, submitted for publication.

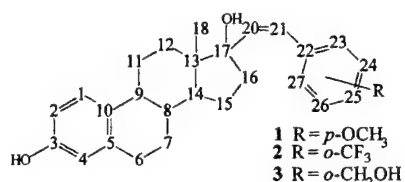


Figure 1. Structures of 1–3.

RBA of 23 in vitro. In stark contrast, (17 $\alpha$ ,20Z)-(o-hydroxymethylphenyl)vinyl estradiol (3) exhibited significant agonist responses with an RBA of 140, giving 3 more potent estrogen binding affinity than estradiol itself.

Previous studies reveal a considerable interest in the conformation of steroids.<sup>7</sup> These studies indicated that the biological activity of these compounds was related to their conformation. Since the placement of a substituent in the *ortho* or *para* positions could affect the conformation and since the conformational characteristics of 17 $\alpha$ -phenylvinyl steroids had not been studied previously, we undertook an investigation of the solution conformation of 1–3. Understanding the preferred conformations is one aspect of an effort to correlate the distinctive biological responses derived from these new probes with their structures and ultimately to associate the responses with the ligand–receptor interactions.

The key conformational feature to establish for 1–3 is the positioning of the 17 $\alpha$  side chain relative to the steroid skeleton. The conformation of the relatively rigid steroid skeleton has been established previously by NMR and other methods.<sup>8</sup> In this study, we use molecular mechanics calculations to generate a set of possible conformations. Two types of NMR data are used in conjunction with the predicted conformations to evaluate which conformations are populated in solution. One approach is to use <sup>13</sup>C chemical shifts in a comparison with shifts predicted for each of the geometries generated from the molecular mechanics calculations. The predicted <sup>13</sup>C shifts come from empirically scaled GIAO (gauge including atomic orbitals) shielding calculations. The other approach is to compare <sup>1</sup>H–<sup>1</sup>H nuclear Overhauser effects established in one- and two-dimensional experiments, 1D and 2D NOESY, with predicted interatomic distances.

**NMR Assignments.** Before NMR data could be used to evaluate the conformations of 1–3, accurate <sup>1</sup>H and <sup>13</sup>C chemical shift assignments were required. The one-dimensional <sup>1</sup>H spectra of 1–3 in acetone-*d*<sub>6</sub> (Figures 2a, 3a, and 4a) reveal that even at 500 MHz, the low-frequency spectral regions (1.2–2.5 ppm) are unassignable directly as a result of the numerous overlapping signals of the 13 protons resonating in this region. In seeking further separation of the low-frequency region, other deuterated solvents were used, namely, benzene,

benzene/acetone, chloroform, chloroform/acetone, and methylene chloride, but pure acetone provides the best separation. Resonances in the low-frequency region that could be readily assigned were the 6 $\alpha$ ,6 $\beta$  benzylic protons near 2.8 ppm and the C18 methyl <sup>1</sup>H signal at 0.9 ppm.<sup>9</sup> Prior literature reports on <sup>1</sup>H NMR assignments of estradiol and other steroids are in disagreement and were of little assistance in assigning the remaining low-frequency region.<sup>10</sup> No publication of <sup>1</sup>H spectral assignments for any 17 $\alpha$ -vinyl-substituted estradiols exists.

The most efficient route to <sup>1</sup>H signal assignment was to first assign the <sup>13</sup>C spectrum. For 1–3, the <sup>13</sup>C experimental shift assignments were based on the study by Dionne and Poirier on <sup>13</sup>C assignments of 17 $\alpha$ -substituted estradiols and our own DEPT and HMBC experiments.<sup>11</sup> The <sup>13</sup>C shift assignments were further supported by theoretical shielding calculations (see below). A heteronuclear multiple quantum coherence (HMQC) experiment was performed to correlate proton signals with directly attached carbons. Because the <sup>1</sup>H chemical shift assignments derived from the HMQC experiment depended on the accuracy of the <sup>13</sup>C chemical shift assignments, other 2D experiments were performed to provide independent evidence. Homonuclear correlation spectroscopy (H,H-COSY) experiments were performed to correlate the assigned <sup>1</sup>H connectivities. The COSY cross-peaks confirmed the initial assignments made by the HMQC experiment. Starting with the unambiguous benzylic H6 signal at 2.8 ppm, the <sup>1</sup>H assignments of the entire aliphatic regions of 1–3 were confirmed.

The HMQC and H,H-COSY experiments clearly indicated the sites of attachment of all of the protons but did not distinguish between the  $\alpha$  and  $\beta$  position of the methylene protons. This distinction was readily achieved by using 2D and 1D nuclear Overhauser effect spectroscopy (NOESY) experiments and by comparing coupling constants. Inspection of the <sup>1</sup>H NMR spectrum allows the axial protons, 7 $\alpha$  and 6 $\beta$ , to be identified by their larger vicinal coupling constants. The equatorial proton, 11 $\alpha$ , is assigned to the isolated signal around 2.4 ppm on the basis of its small coupling constants. The remaining  $\beta$  protons were assigned by the determination of transient NOEs using a 1D NOESY experiment, the 1D analogue of the 2D NOESY experiment.<sup>12</sup> The 1D NOESY experiment avoided problems associated with imperfect subtraction in NOE difference experiments.<sup>13</sup>

Using a selective Gaussian pulse, irradiation of the C18 methyl peaks of 1–3 gave signal enhancements for the  $\beta$ -protons at positions 8, 11, 12, 15, and 16 (Figures 2b, 3b, and 4b). These experiments were crucial in making chemical shift assignments, since they resolved  $\beta$  protons from overlapping regions containing  $\alpha$  protons. For example, the spectrum of 2 shows a set of four overlapping protons at  $\delta$  1.65–1.8 for 12 $\alpha$ , 12 $\beta$ , H14 and 15 $\alpha$ .

(7) (a) Duax, W. L.; Cody, V.; Griffin, J. F.; Hazel, J.; Weeks, C. M. *J. Steroid Biochem.* **1978**, *9*, 901. (b) Duax, W. L.; Cody, V.; Hazel, J. *Steroids* **1977**, *30*, 471. (c) Duax, W. L.; Weeks, C. M.; Rohrer, D. C.; Osawa, Y.; Wolff, M. E. *J. Steroid Biochem.* **1975**, *6*, 195. (d) Precigoux, G.; Busetta, B.; Courseille, C.; Hospital, M. *Acta Crystallogr., Sect. B* **1975**, *31*, 1527. (e) Kim, R. S.; Labella, F. S.; Zunza, H.; Zunza, F.; Templeton, J. F. *Mol. Pharmacol.* **1980**, *18*, 395.

(8) (a) Marat, K.; Templeton, J. F.; Kumar, V. P. S. *Magn. Reson. Chem.* **1986**, *25*, 25. (b) Barrett, M. W.; Farrant, D. N.; Krik, D. N.; Mersh, J. D.; Sanders, J. K. M.; Duax, W. L. *J. Chem. Soc., Perkin Trans. 1* **1977**, *30*, 471. (c) Kollman, P. A.; Giannini, D. D.; Duax, W. L.; Rothenberg, S.; Wolff, M. E. *J. Am. Chem. Soc.* **1973**, *95*, 2865. (d) Osawa, Y.; Gardner, J. O. *J. Org. Chem.* **1971**, *36*, 3246.

(9) Kirk, D. N.; Toms, H. C.; Douglas, C.; White, K. A.; Smith, K. E.; Latif, S.; Hubbard, R. W. P. *J. Chem. Soc., Perkins Trans. 2* **1990**, *2*, 10.

(10) (a) Kayser, F.; Biesemans, M.; Pan, H.; Gielen, M.; Willem, R.; Kumar, S.; Schneider, H. *J. J. Chem. Soc., Perkins Trans. 2* **1989**, *2*, 245. (b) Savignac, M.; Jaouen, G.; Rodger, C. A.; Perrier, R. E.; Sayer, B. G.; McGlinchey, M. *J. J. Org. Chem.* **1986**, *51*, 2328. (c) Sedee, A. G.; Henegouwen, M. *J. J. Chem. Soc., Perkins Trans. 2* **1984**, *2*, 1755.

(11) Dionne, P.; Poirier, P. *Steroids* **1995**, *60*, 830.

(12) Kessler, H.; Oschkinat, H.; Griesinger, C.; Bermel, W. *J. Magn. Reson.* **1986**, *70*, 106–133.

(13) Toffanin, R.; Matulova, M.; Bella, J.; Lamba, D.; Cescutti, P.; Paoletti, S.; Kvam, B. *J. Carbohydr. Res.* **1994**, *265*, 151.

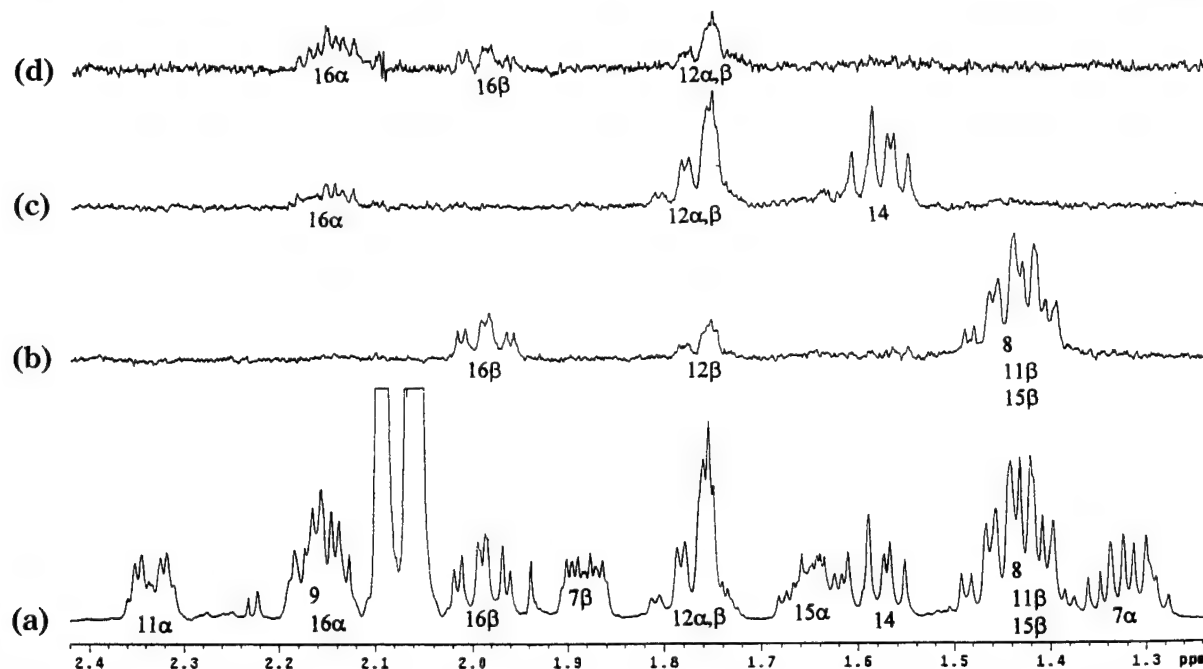


**Figure 2.** (a) Low-frequency spectral region of the 500 MHz  $^1\text{H}$  NMR spectra of **1** in acetone- $d_6$ . Equivalent spectral regions of the 500 MHz 1D NOESY spectra (500 ms mixing time) of **1** obtained by selective irradiation of the C18 methyl (b), H<sub>2</sub>O (c), and H<sub>23/27</sub> (d) using a Gaussian pulse. Spectra b and c are 5 $\times$  the vertical scale of a. Spectra d is 10 $\times$  the vertical scale of a.

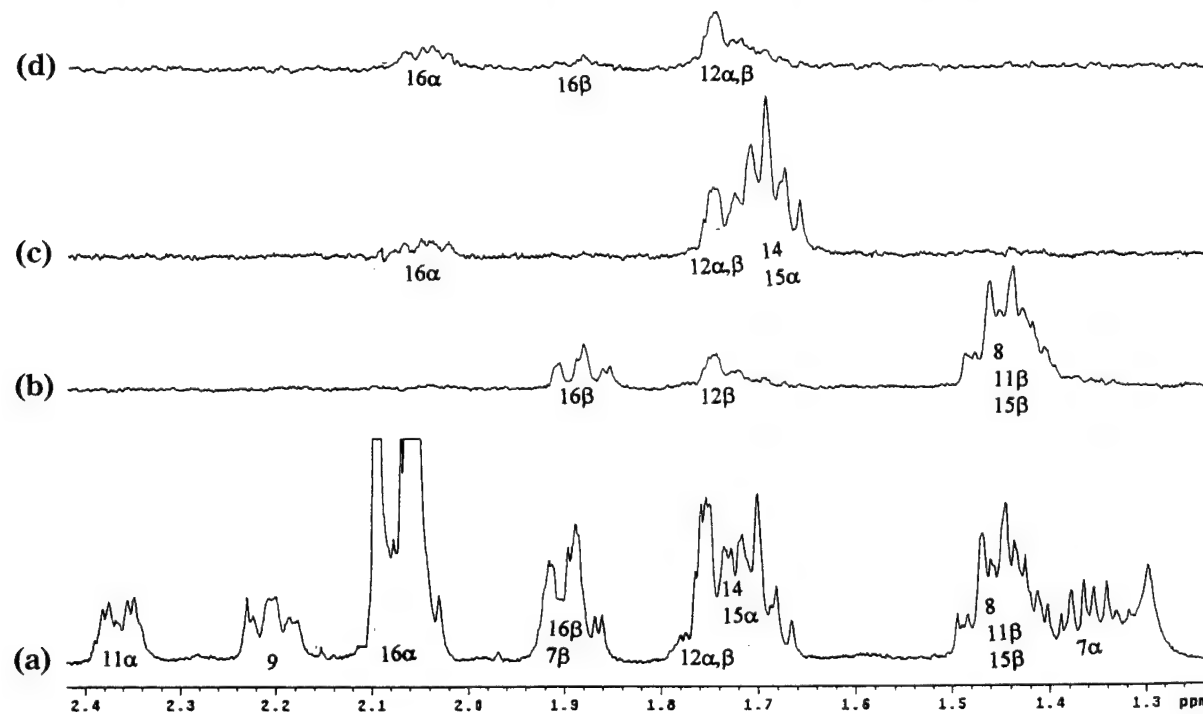


**Figure 3.** (a) Low-frequency spectral region of the 500 MHz  $^1\text{H}$  NMR spectra of **2** in acetone- $d_6$ . Equivalent spectral regions of the 500 MHz 1D NOESY spectra (500 ms mixing time) of **2** obtained by selective irradiation of the C18 methyl (b), H<sub>2</sub>O (c), and H<sub>27</sub> (d) using a Gaussian pulse. Spectra b and c are 5 $\times$  the vertical scale of a. Spectra d is 10 $\times$  the vertical scale of a.

Irradiation of the C18 methyl, in the 1D NOESY experiment, reveals at 1.75 ppm the expected  $12\beta$  signal from the overlapping region. The remaining assignments in this set are based on the HMQC of steroid **2** that shows that the H<sub>14</sub> and 15 $\alpha$  protons are slightly further upfield (1.7 and 1.72 ppm) than 12 $\alpha$  or  $12\beta$ . The remaining signal at 1.77 ppm can therefore be assigned to 12 $\alpha$ . Assignments in the B and C ring were validated by other 1D NOESY experiments, including the irradiation of H<sub>1</sub> that

results in the expected enhancement of 11 $\alpha$  and the irradiation of H<sub>6</sub>, yielding the expected 7 $\alpha$ , 7 $\beta$ , and H<sub>8</sub> enhancements. In summary, consideration of all the independent NMR experiments allowed the unambiguous assignment of all  $^1\text{H}$  and  $^{13}\text{C}$  resonances. Table 1 summarizes all of the  $^1\text{H}$  and  $^{13}\text{C}$  chemical shifts for **1–3**.

**Theoretical Carbon Chemical Shifts and Solution Conformations.** The predicted low-energy conformers of **1–3** were generated using the MM3 force field and

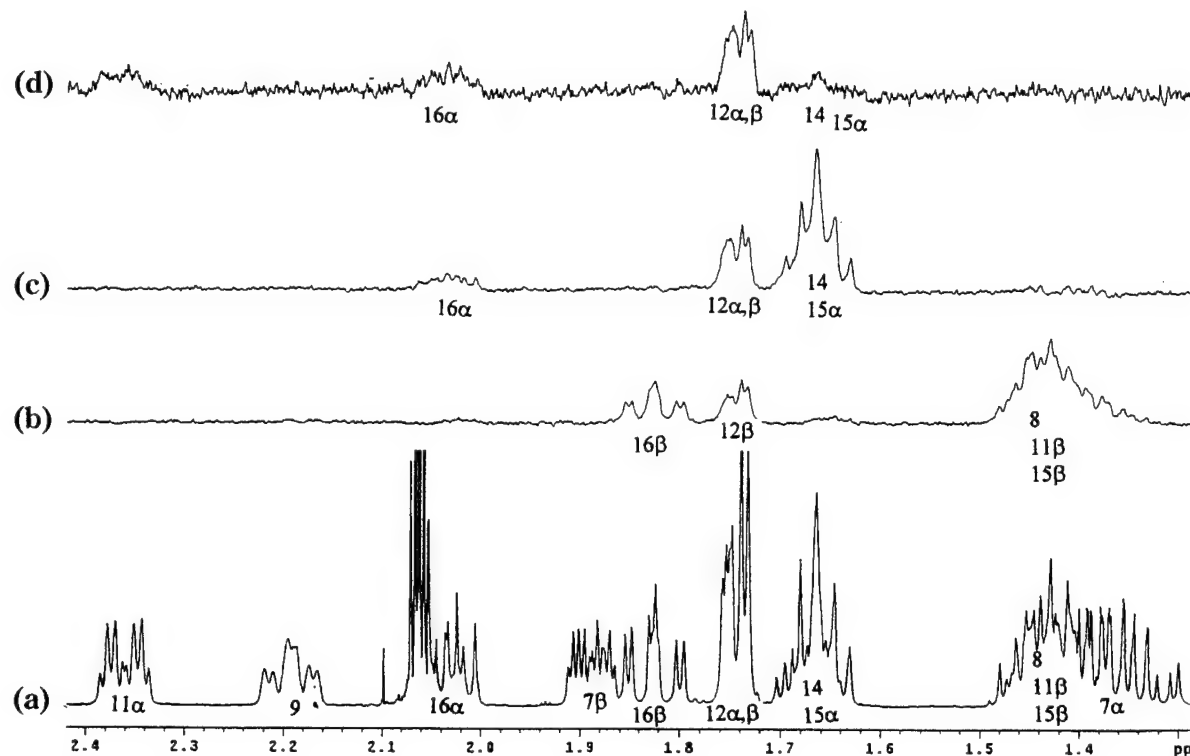


**Figure 4.** (a) Low-frequency spectral region of the 500 MHz  $^1\text{H}$  NMR spectra of **3** in acetone- $d_6$ . Equivalent spectral regions of the 500 MHz 1D NOESY spectra (500 ms mixing time) of **3** obtained by selective irradiation of the C18 methyl (b), H<sub>2</sub>O (c), and H<sub>23/27</sub> (d) using a Gaussian pulse. Spectra b and c are 5 $\times$  the vertical scale of a. Spectra d is 15 $\times$  the vertical scale of a.

**Table 1.**  $^1\text{H}$  and  $^{13}\text{C}$  Chemical Shifts for **1–3**

$^1\text{H}$	1	2	3	$^{13}\text{C}$	1	2	3
1	7.12	7.12	7.12	1	126.9	127.4	126.5
2	6.60	6.62	6.62	2	113.5	113.9	113.2
4	6.54	6.60	6.58	3	155.8	155.0	153.2
6 $\alpha$	2.75	2.78	2.79	4	115.8	116.2	115.2
6 $\beta$	2.80	2.81	2.82	5	138.3	139.1	137.5
7 $\alpha$	1.32	1.38	1.34	6	29.9	30.7	29.8
7 $\beta$	1.88	1.88	1.88	7	28.5	28.7	27.9
8	1.43	1.48	1.43	8	40.7	41.2	40.2
9	2.18	2.20	2.18	9	44.5	45.0	44.0
11 $\alpha$	2.33	2.38	2.36	10	131.9	131.9	131.9
11 $\beta$	1.46	1.45	1.46	11	27.3	27.7	26.8
12 $\alpha$	1.77	1.77	1.76	12	32.6	33.7	33.0
12 $\beta$	1.75	1.75	1.74	13	48.7	49.0	48.0
14	1.57	1.70	1.66	14	49.9	50.8	49.9
15 $\alpha$	1.64	1.72	1.68	15	23.7	24.4	23.4
15 $\beta$	1.41	1.43	1.40	16	38.3	39.3	38.4
16 $\alpha$	2.16	2.06	2.02	17	83.8	85.8	84.8
16 $\beta$	1.98	1.90	1.82	18	14.5	14.8	14.6
CH <sub>3</sub>	0.96	0.90	0.88	20	135.1	138.7	138.0
20	5.88	6.10	6.03	21	129.7	124.2	125.0
21	6.39	6.59	6.50	22	130.5	137.8	138.2
23	7.63	N/A	N/A	23	132.4	133.3	138.5
24	6.86	7.61	7.36	24	113.6	125.9	129.0
25	N/A	7.52	7.20	25	159.4	131.9	126.8
26	6.86	7.39	7.18	26	113.6	130.5	127.8
27	7.63	7.64	7.21	27	132.4	132.3	126.8
28 <sup>a</sup>	3.80	N/A	4.60	28 <sup>a</sup>	55.3	127.6	62.5

<sup>a</sup> Additional alkyl: 1, OCH<sub>3</sub>; 2, CF<sub>3</sub>; 3, CH<sub>2</sub>OH.

were initially determined by rotation around dihedrals C13–C17–C20–C21 and C20–C21–C22–C23 (Figures 5–7).<sup>14</sup> The OH and OCH<sub>3</sub> groups were then rotated so as to find the lowest energy position. For **3**, hydrogen bonding between the 17-OH and 23-CH<sub>2</sub>OH group resulted in three pairs (**3a/3c**, **3b/3d**, **3e/3f**) of proton donor/

acceptor conformers. The key dihedral angles for the lowest energy conformers, **1a–e**, **2a–f**, and **3a–h**, with energies within 6 kcal of the lowest energy conformer for **1–3**, are listed in Table 2. Conformers **1d**, **2d**, **3e**, and **3f**, which have an orthogonal alignment between the estradiol skeleton and the 17 $\alpha$  substituent and an anti alignment between the phenyl ring and the C18 methyl, are referred to herein as anti orthogonal conformers. Conversely, conformers **1a**, **2a**, **3a**, and **3c** will be referred to as syn orthogonal conformers. Conformers **1b**, **2b**, **2c**, **3b**, **3d**, and **3h** are designated as extended conformers. All other conformers will be described via a combination of these names.

As the MM3 calculations show, significant changes in the 17 $\alpha$  side chain conformation result in minor energy differences. In fact, most of the low-energy conformers are within 3 kcal of the lowest energy conformer. This made any conformational determination based purely on energy predictions unreliable.

More reliable conclusions regarding the 17 $\alpha$  side chain conformation of **1–3** could be achieved by comparing predicted  $^{13}\text{C}$  chemical shifts for each MM3 conformer to experimental shifts. These predicted  $^{13}\text{C}$  chemical shifts,  $\delta_{\text{pred}}$ , were calculated by empirically scaling GIAO-calculated absolute shieldings,  $\sigma$ .<sup>15</sup> The appropriate scaling equation depends on the basis set. In this study, in which GIAO shielding calculations were obtained at the B3LYP/3-21G level with heteroatoms augmented at the 6-31+G\* level, the appropriate scaling is given by eq 1,

$$\delta_{\text{pred}} = -1.168\sigma + 230.2 \quad (1)$$

(14) (a) Allinger, N. L.; Yuh, Y. H.; Lii, J. H. *J. Am. Chem. Soc.* **1989**, *111*, 8551, 8566, 8576. (b) MM3(94); Tripos, Inc.: St. Louis, MO.

(15) (a) Ditchfield, R. *Mol. Phys.* **1974**, *27*, 789. (b) Rohling, C. M.; Allen, L. C.; Ditchfield, R. *Chem. Phys.* **1984**, *87*, 9. (c) Wolinski, K.; Hinton, J. F.; Pulay, P. *J. Am. Chem. Soc.* **1990**, *112*, 8251.

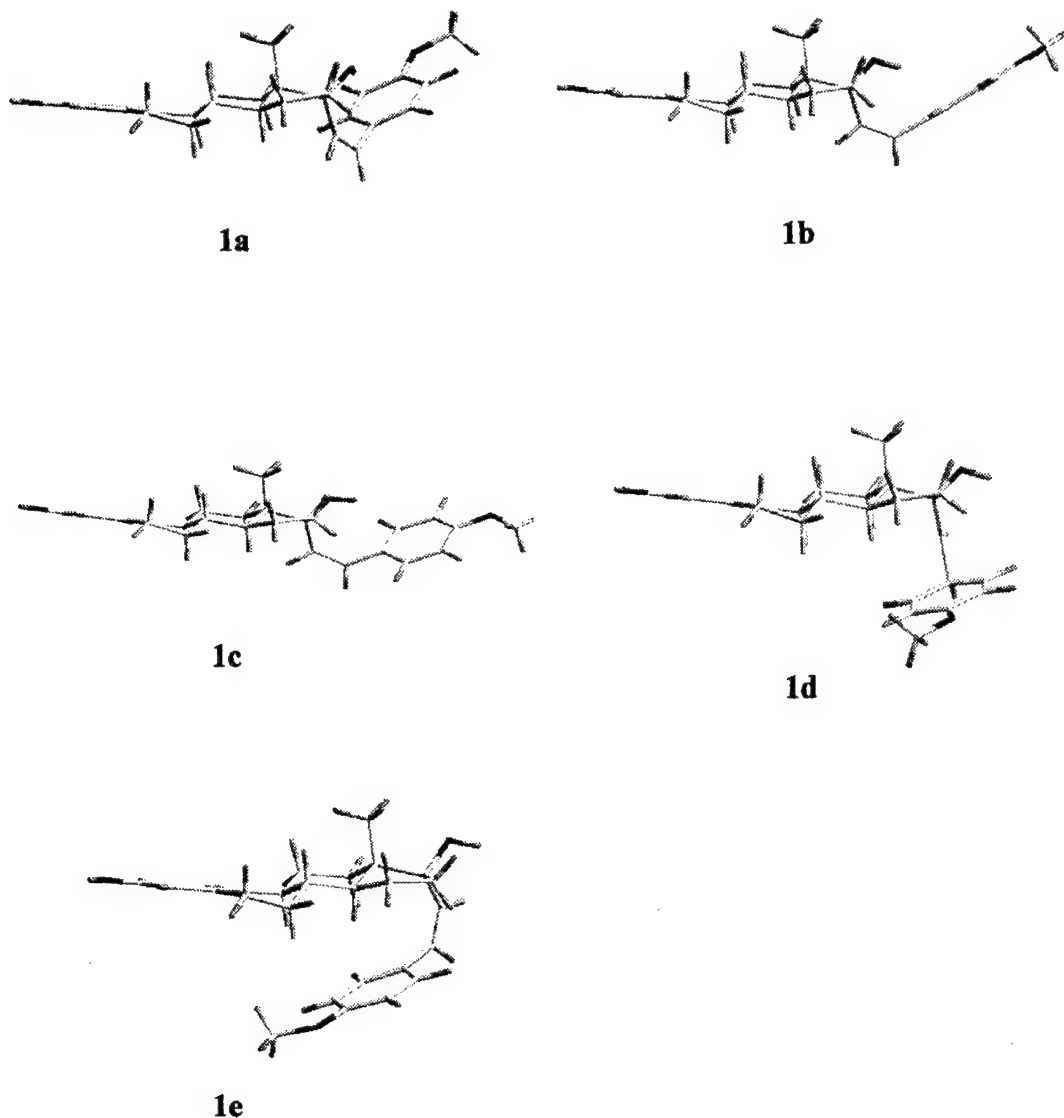


Figure 5. MM3-predicted geometries for the most stable conformers of 1.

as determined previously.<sup>16</sup> All calculations were carried out with the Gaussian 98 program.<sup>17</sup> Tables 3–5 list the predicted <sup>13</sup>C chemical shifts of each MM3 conformer and the assigned experimental <sup>13</sup>C chemical shifts for 1–3.

Previously, Dionne and Poirier showed that the carbons in the A, B, and C ring experience little shielding or deshielding effects from various 17 $\alpha$  substituents since these carbons exhibit minor ( $\sim$ 1 ppm) chemical shift changes. However, carbons in the D ring were significantly influenced by various 17 $\alpha$  substituents. Specifically, C16 and C17 were shown to be the most heavily influenced. Our predicted <sup>13</sup>C chemical shifts correspond

quite well with the carbons in rings A, B, and C (C1–C14); in fact, most of the <sup>13</sup>C predictions in rings A, B, and C are within 1 ppm of the assigned experimental values. These results demonstrate the accuracy of these predictions in an area of a well-defined geometry without any conformational distinction. The shielding and deshielding effects of the 17 $\alpha$  substituent are clearly evident in the predicted chemical shift of C16 in different conformers of 1. In conformers 1b and 1e, respectively the second lowest and the highest energy conformers of 1, the predicted shifts of C16 differ by more than 8 ppm from the experimental value. Similarly for 2 and 3, the predicted <sup>13</sup>C chemical shifts of C16 differ from the observed shift by more than 4 ppm for conformer 2d and 5 ppm for conformers 2b, 3f, and 3h. These large differences of the predicted shifts of C16 among similar conformers are attributed to the steric interactions between the ortho protons H23/27 and 16 $\alpha$ . For example, the predicted C16 shift for extended conformer 1b with a spatial distance between H23/27 and 16 $\alpha$  of 2.2 D differs from experiment by more than 8 ppm, while the C16 shift prediction for anti orthogonal/extended conformer 1c with a distance between H23/27 and 16 $\alpha$  of 3.2 D is within 1 ppm of the experimental value.

(16) Forsyth, D. A.; Sebag, A. B. *J. Am. Chem. Soc.* 1997, 119, 9483.  
 (17) Gaussian 98, Revision A.3; Frisch, M. J.; Trucks, G. W.; Schlegel, H. B.; Scuseria, G. E.; Robb, M. A.; Cheeseman, J. R.; Zakrzewski, V. G.; Montgomery, J. A., Jr.; Stratmann, R. E.; Burant, J. C.; Dapprich, S.; Millam, J. M.; Daniels, A. D.; Kudin, K. N.; Strain, M. C.; Farkas, O.; Tomasi, J.; Barone, V.; Cossi, M.; Cammi, R.; Mennucci, B.; Pomelli, C.; Adamo, C.; Clifford, S.; Ochterski, J.; Petersson, G. A.; Ayala, P. Y.; Cui, Q.; Morokuma, K.; Malick, D. K.; Rabuck, A. D.; Raghavachari, K.; Foresman, J. B.; Cioslowski, J.; Ortiz, J. V.; Stefanov, B. B.; Liu, G.; Liashenko, A.; Piskorz, P.; Komaromi, I.; Gomperts, R.; Martin, R. L.; Fox, D. J.; Keith, T.; Al-Laham, M. A.; Peng, C. Y.; Nanayakkara, A.; Gonzalez, C.; Challacombe, M.; Gill, P. M. W.; Johnson, B.; Chen, W.; Wong, M. W.; Andres, J. L.; Gonzalez, C.; Head-Gordon, M.; Replogle, E. S.; Pople, J. A. Gaussian, Inc., Pittsburgh, PA, 1998.

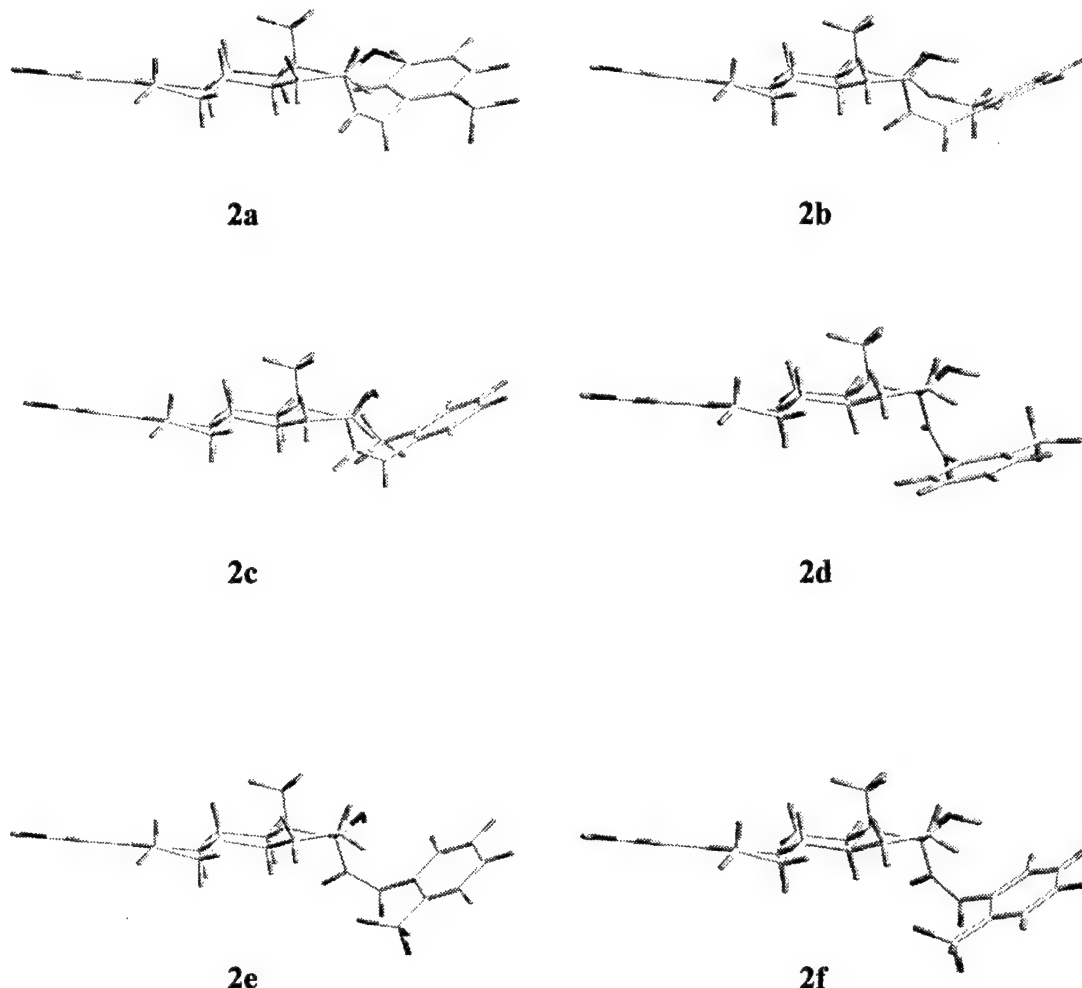


**Figure 6.** MM3-predicted geometries for the most stable conformers of **2**.

If **1–3** are rapidly exchanging among conformers, only average positions of the  $^{13}\text{C}$  resonances will be observed experimentally on the NMR time scale. To determine the contributing conformers of **1–3**, we chose a statistical approach in which the predicted  $^{13}\text{C}$  shifts of the C and D rings of all reasonable conformers of **1–3** were in each separate case treated as independent variables in a multiple independent variable regression analysis of the corresponding experimental data.<sup>18</sup> The predicted  $^{13}\text{C}$  shifts of the A and B rings of all reasonable conformers of **1–3** were not used in this statistical analysis since they are all within 1 ppm of the experimental values regardless of the conformer. The regression analysis yielded fractional populations as the fitting parameters. All standard errors and confidence levels of the regression analysis were estimated using the Bootstrapping method.<sup>19</sup> The results and corresponding estimates of uncertainties (standard errors) are listed in Table 6. Both **1** and **2** were found to have a major conformer, **1c** 68(24)% and **2c** 60-(1)%. Two minor conformers are also indicated for each: **1a** 20(12)% and **1d** 12(30)%, and **2a** 20(13)% and **2f** 20-(8)%. For **3**, conformers **3a** 36(14)%, **3d** 34(26)%, and **3e** 28(14)% were found to be similarly populated. It is important to note that the large corresponding standard error of certain contributing conformers renders conclu-

sions on their presence unreliable. This is evident with predicted conformer **1d** that is estimated to be 12% present but has a 30% standard error.

**NOESY Studies.** The solution state conformations of the  $17\alpha$  side chain of **1–3** were also probed by 2D and 1D NOESY experiments. In the case of **1**, the low-frequency region of the 2D NOESY spectrum reveals strong cross-peaks involving the vinyl proton,  $\text{H}_{20}$ , with  $\text{H}_{14}$  and  $12\alpha,\beta$ . A weaker cross-peak with  $16\alpha$  could also be detected. The 2D NOESY spectrum also reveals weak cross-peaks between the  $\text{H}_{23/27}$  aryl protons and four alkyl protons,  $12\alpha$ ,  $12\beta$ ,  $16\alpha$ , and  $16\beta$ . The NOE data provide evidence for more than one conformer since no single conformer of **1** is expected to have an NOE with either  $\text{H}_{23}$  or  $\text{H}_{27}$  and both  $12\alpha$  and  $16\alpha$ . As all of the predicted low-energy conformers of **1** show, structures with a distance between  $\text{H}_{23}$  or  $\text{H}_{27}$  and  $12\alpha$  appropriate for an NOE preclude an NOE with  $16\alpha$  as a result of too great of a distance ( $>5$  Å). Conformer **1c**, for example, which has a distance between  $\text{H}_{27}$  and  $16\alpha$  of 3.2 Å, has a distance greater than 5 Å between  $\text{H}_{23}$  or  $\text{H}_{27}$  and  $12\alpha$ .

In keeping with the 2D NOESY results for **1**, the selective 1D NOESY of  $\text{H}_{20}$  reveals equally strong enhancements of  $12\alpha,\beta$  and  $\text{H}_{14}$  and a weak enhancement of  $16\alpha$  (Figure 2c). Similarly, the 1D NOESY of  $\text{H}_{23/27}$  shows weak enhancement of  $12\alpha$ ,  $12\beta$ ,  $16\alpha$ , and  $16\beta$  (Figure 2d). Comparison of the intensity of these enhancements suggests a similarly short distance be-

(18) SPSS, V. 10, SPSS Inc.: Chicago, IL.

(19) Mooney C. Z.; Duval R. D. *Bootstrapping*; Sage Publications: Newbury Park, CA, 1993.

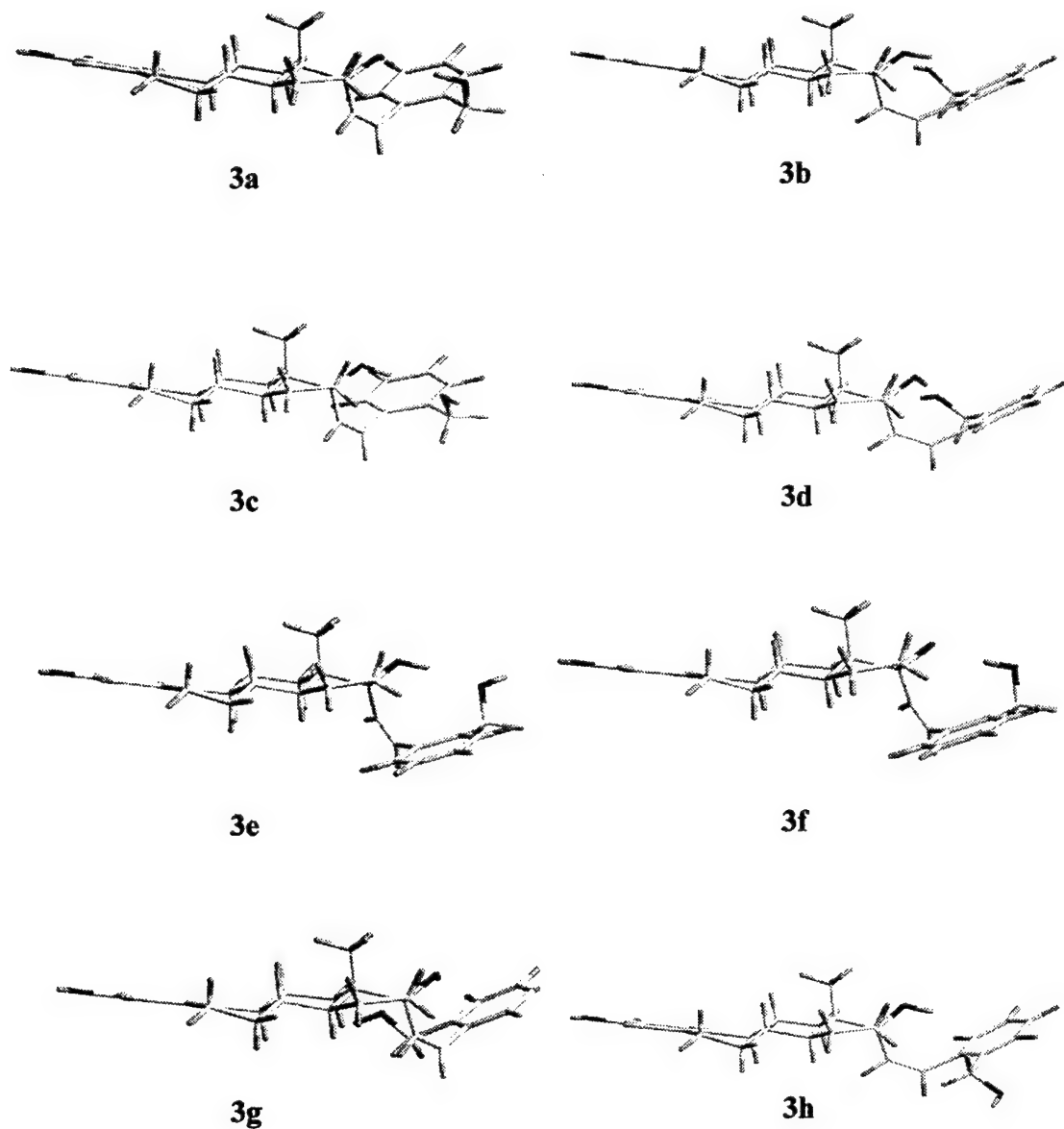


**Figure 7.** MM3-predicted geometries for the most stable conformers of 3.

**Table 2. Relative Energies and Key Dihedrals of Predicted Conformers of 1–3 Using MM3**

conformers	C13–C17–C20–C21	C20–21–22–23	rel energies (kcal/mol)
1a	-103	-86	0
1b	-156	-68	0.6
1c	-110	-110	3
1d	105	86	3.2
1e	70	81	5.7
2a	-112	-99	0
2b	-151	109	0.3
2c	-148	93	1.7
2d	118	85	2.1
2e	162	-125	2.3
2f	145	-118	3.1
3a	106	90	0
3b	155	98	0.6
3c	109	94	2.3
3d	150	78	2.6
3e	-131	-81	3.3
3f	-132	-81	3.7
3g	111	105	4.2
3h	153	89	4.9

tween H20 and 12 $\alpha,\beta$  and between H20 and H14, as well as greater distances between H20 and 16 $\alpha$  and between H23/27 and 12 $\alpha$ , 12 $\beta$ , 16 $\alpha$ , and 16 $\beta$ . Table 7 summarizes

and compares the intensity of the observed NOE signals with expected NOEs based on H–H distances in all predicted low-energy conformers of 1. Comparison of these observed enhancements with expected NOE intensities for all predicted low-energy conformers of 1 rules out conformers 1d and 1e as contributing conformers based on the absence of observable NOE signals involving H23/27 with H14 and 15 $\alpha$ . The strong, equally enhanced NOE signals between H20 and 12 $\alpha$  and between H20 and H14 suggest that the major conformer bears an extended side chain geometry, consistent with conformers 1b and 1c. In comparing conformers 1b and 1c, the weak NOE signal between H23/27 and 16 $\alpha$  is consistent with the expected weak NOE intensity between H23/27 and 16 $\alpha$  of conformer 1c and inconsistent with the expected strong NOE intensity between H27 and 16 $\alpha$  of conformer 1b. Therefore, conformer 1c is considered the major conformer.

The weak NOE signal between H23/27 and 12 $\alpha,\beta$ , which is not expected to arise from conformers 1b or 1c since these conformers have distances greater than 5 Å

**Table 3. Experimental and Predicted  $^{13}\text{C}$  Chemical Shifts (ppm) of Predicted Conformers of **1** Using B3LYP/3-21G(X,6-31+G\*)//MM3 Calculations**

	<b>1a</b>	<b>1b</b>	<b>1c</b>	<b>1d</b>	<b>1e</b>	expt
C1	127.5	127.6	127.5	127.5	127.4	126.9
C2	113.0	113.0	113.1	113.0	112.8	113.5
C3	152.9	152.9	153.0	152.9	152.6	155.8
C4	115.6	115.6	115.7	115.6	115.7	115.8
C5	136.3	136.2	136.1	136.1	136.1	138.3
C6	31.0	31.1	31.1	31.0	30.7	29.9
C7	28.4	28.4	28.4	28.5	27.0	28.5
C8	40.1	39.8	39.7	39.6	38.7	40.7
C9	44.3	44.4	44.3	44.3	42.5	44.5
C10	132.1	132.1	132.2	132.3	132.3	131.9
C11	28.5	28.4	28.5	28.5	28.5	27.3
C12	34.2	32.0	31.9	32.8	34.0	32.6
C13	48.6	48.0	47.6	48.4	49.8	48.7
C14	50.7	48.7	49.1	49.0	47.3	49.9
C15	26.0	26.8	26.1	25.3	27.1	23.7
C16	39.8	46.6	38.1	37.5	46.6	38.3
C17	86.1	83.4	79.7	83.0	86.1	83.8
C18	16.0	15.3	14.3	15.1	16.1	14.5
C20	142.2	144.5	142.4	142.9	152.0	135.1
C21	133.1	130.8	134.8	135.3	134.5	129.7
C22	127.8	129.6	130.4	129.5	132.1	130.5
C23	129.2	130.1	127.4	131.7	129.1	132.4
C24	117.1	118.8	119.2	117.1	118.7	113.6
C25	157.5	157.5	157.6	156.9	157.4	159.4
C26	109.4	110.0	110.8	109.2	110.1	113.6
C27	132.2	128.6	128.8	129.6	130.9	132.4
C28	54.0	54.0	54.6	54.0	54.5	55.3

**Table 4. Experimental and Predicted  $^{13}\text{C}$  Chemical Shifts (ppm) of Predicted Conformers of **2** Using B3LYP/3-21G(X,6-31+G\*)//MM3 Calculations**

	<b>2a</b>	<b>2b</b>	<b>2c</b>	<b>2d</b>	<b>2e</b>	<b>2f</b>	expt
C1	127.3	127.6	127.6	127.5	127.6	127.4	127.4
C2	113.0	113.1	113.1	113.0	113.0	113.0	113.9
C3	153.0	153.0	152.9	153.0	152.9	153.2	155.0
C4	115.9	115.8	115.6	115.7	115.8	115.7	116.2
C5	136.0	136.0	135.9	136.1	136.3	136.3	139.1
C6	30.9	31.0	30.9	31.1	31.1	31.1	30.7
C7	28.3	28.4	28.4	28.4	28.1	28.0	28.7
C8	39.7	39.7	40.0	39.8	39.9	40.1	41.2
C9	44.1	44.0	44.4	44.1	43.9	44.0	45.0
C10	131.9	132.1	132.1	132.0	131.9	132.0	131.9
C11	28.5	28.4	28.3	28.6	28.4	28.6	27.7
C12	34.9	32.1	33.9	32.3	30.8	30.9	33.7
C13	48.0	47.9	49.3	48.0	47.7	48.0	49.0
C14	50.1	49.5	50.5	49.1	49.1	48.7	50.8
C15	26.5	26.8	26.3	26.3	25.8	26.1	24.4
C16	42.6	45.1	39.3	35.0	40.6	36.1	39.3
C17	86.1	84.4	87.8	81.8	81.8	80.5	85.8
C18	14.6	15.1	16.1	14.7	15.4	15.0	14.8
C20	143.7	147.0	141.6	142.0	145.5	140.6	138.7
C21	127.8	126.2	129.2	129.4	132.0	133.3	124.2
C22	138.9	138.9	135.5	139.8	139.2	140.5	137.8
C23	129.2	133.4	131.5	132.4	131.1	130.5	133.3
C24	125.9	127.2	127.4	126.6	129.2	128.1	125.9
C25	130.7	128.8	131.1	130.6	130.8	130.4	131.9
C26	131.7	131.0	130.2	131.4	132.0	131.7	130.5
C27	132.2	128.8	134.5	129.4	129.6	130.8	132.3
C28	127.0	127.1	127.4	126.7	127.3	127.0	127.6

between H23/27 and 12 $\alpha$ , $\beta$ , supports the presence of the syn orthogonal conformer **1a**.

In regard to conformations for **2**, the low-frequency region of the 2D NOESY spectrum of **2** displays a strong cross-peak between H20 and an overlapping region consisting of 12 $\alpha$ , 12 $\beta$ , H14, and 15 $\alpha$ . Additionally, weak cross-peaks between H27 and 12 $\alpha$ , $\beta$ , 16 $\alpha$ , and 16 $\beta$  are observable. This pattern of NOESY cross-peaks is similar to that observed for **1**. An additional weak cross-peak between H21 and 12 $\alpha$ , $\beta$  could also be detected. A selective 1D NOESY of H20 reveals that the strong cross-peak

**Table 5. Experimental and Predicted  $^{13}\text{C}$  Chemical Shifts (ppm) of Predicted Conformers of **3** Using B3LYP/3-21G(X,6-31+G\*)//MM3 Calculations**

	<b>3a</b>	<b>3b</b>	<b>3c</b>	<b>3d</b>	<b>3e</b>	<b>3f</b>	<b>3g</b>	<b>3h</b>	expt
C1	127.4	127.6	127.4	127.4	127.5	127.3	127.3	127.3	126.5
C2	113.1	113.2	112.9	112.9	112.8	112.9	112.9	113.0	113.2
C3	153.1	153.0	152.8	152.9	152.8	153.1	152.9	152.9	153.2
C4	115.9	115.7	115.7	115.7	115.6	115.8	115.7	115.8	115.2
C5	136.0	136.0	136.1	136.3	136.3	136.3	136.1	136.1	137.5
C6	30.9	31.0	31.0	31.1	31.2	31.0	31.1	31.0	29.8
C7	28.2	28.5	28.4	28.5	28.3	28.1	28.5	28.4	27.9
C8	39.8	39.7	39.6	40.0	40.0	40.1	40.1	39.6	40.2
C9	44.0	44.1	44.1	44.2	44.0	43.8	44.5	44.3	44.0
C10	131.7	131.8	132.5	132.3	132.4	131.4	132.2	132.1	131.9
C11	28.4	28.3	28.6	28.5	28.7	28.4	28.6	28.5	26.8
C12	34.3	31.3	34.9	31.9	31.7	30.4	33.0	32.3	33.0
C13	48.0	47.5	47.8	48.0	47.7	48.1	49.1	48.3	48.0
C14	50.4	49.2	50.1	49.2	49.3	49.1	50.8	49.3	49.9
C15	26.2	26.6	26.8	26.1	25.7	25.0	26.2	26.7	23.4
C16	39.4	44.9	43.3	42.0	34.4	30.9	39.2	43.6	38.4
C17	85.9	83.3	85.4	84.4	79.9	80.2	87.3	85.8	84.8
C18	16.1	15.3	14.7	16.0	15.5	15.4	16.0	14.9	14.6
C20	141.6	144.6	145.0	146.1	142.8	136.2	141.7	141.5	138.0
C21	130.9	129.6	128.3	127.8	129.2	136.5	130.5	127.8	125.0
C22	134.5	136.4	140.2	140.6	140.5	135.5	133.4	134.3	138.2
C23	141.0	140.6	133.2	133.5	135.9	140.4	136.4	140.0	138.5
C24	131.9	131.7	131.4	131.2	132.5	131.8	130.0	130.4	129.0
C25	128.5	126.8	128.5	126.9	126.9	127.9	127.7	127.9	126.8
C26	126.0	128.3	127.0	128.8	128.3	126.2	126.2	126.6	127.8
C27	131.9	131.7	131.4	131.2	127.7	131.8	132.8	126.5	126.8
C28	64.5	65.0	65.9	66.2	64.7	64.1	63.2	63.3	62.5

**Table 6. Summary of the Multiple Independent Variable Regression Analysis<sup>a</sup> of the Calculated  $^{13}\text{C}$  Shifts of Predicted Conformers of **1–3****

conformer	estimate (%)	standard error (%)
<b>1a</b>	20	12
<b>1b</b>	0	7
<b>1c</b>	68	24
<b>1d</b>	12	30
<b>1e</b>	0	0
<b>2a</b>	20	13
<b>2b</b>	0	15
<b>2c</b>	60	1
<b>2d</b>	0	7
<b>2e</b>	0	11
<b>2f</b>	20	8
<b>3a</b>	36	14
<b>3b</b>	0	1
<b>3c</b>	0	5
<b>3d</b>	34	26
<b>3e</b>	28	14
<b>3f</b>	0	1
<b>3g</b>	2	7
<b>3h</b>	0	10

<sup>a</sup> Constraints: Each conformer is greater than or equal to 0%. Conformer sets **1a–e**, **2a–f**, and **3a–h** are equal to 100%.

consists mainly of signal from H14 with some contribution from 12 $\alpha$ , $\beta$  (Figure 3c). The 1D NOESY of H20 also displays a very weak enhancement of 16 $\alpha$ . The 1D NOESY of H27 displays the expected weak enhancements of 12 $\alpha$ , $\beta$ , 16 $\alpha$ , and 16 $\beta$  expected from the 2D NOESY experiment (Figure 3d). The NOE data indicates the presence of at least two conformers with rotated phenyl rings since no predicted conformer of **2** is expected to have an NOE with H27 and both 12 $\alpha$  and 16 $\beta$ .

As described in detail below, comparing these observed enhancements with expected NOE intensities for predicted conformers of **2** suggests that conformer **2c** is the major conformer with minor contribution from **2a** and other conformers as well (see Table 8).

**Table 7. Summary and Comparison of Observed NOE Enhancements with Expected NOE Intensities<sup>a</sup> for Predicted Conformers of 1**

irradiated	enhanced	1a	1b	1c	1d	1e	expt
H20	12 $\alpha,\beta$	w	s	s	s	w	s
H20	H14	s	s	s	w	w	s
H20	16 $\alpha$	s	w	w	w	w	w
H23/27	12 $\alpha,\beta$	s	n	n	w	s	w
H23/27	H14	n	n	n	s	s	n
H23/27	15 $\alpha$	n	n	n	w	s	n
H23/27	16 $\alpha$	n	s	w	s	s	w
H23/27	16 $\beta$	n	w	w	w	s	w

<sup>a</sup> Expectations of strong (s), weak (w), and no (n) NOE enhancements correspond to H–H distances of 0–2.99, 3.0–4.99, and >5 Å.

**Table 8. Summary and Comparison of Observed NOE Enhancements with Expected NOE Intensities<sup>a</sup> for Predicted Conformers of 2**

irradiated	enhanced	2a	2b	2c	2d	2e	2f	expt
H20	12 $\alpha,\beta$	w	s	s	s	s	s	s
H20	H14	s	s	s	w	s	w	s
H20	16 $\alpha$	s	w	w	w	w	w	w
H21	12 $\alpha,\beta$	w	n	n	n	n	n	w
H27	12 $\alpha,\beta$	s	n	n	w	n	n	w
H27	H14	n	n	n	s	n	n	n
H27	15 $\alpha$	n	n	n	s	n	n	n
H27	16 $\alpha$	n	s	w	w	n	s	w
H27	16 $\beta$	n	w	w	n	w	w	w

<sup>a</sup> Expectations of strong (s), weak (w), and no (n) NOE enhancements correspond to H–H distances of 0–2.99, 3.0–4.99, and >5 Å.

The observed strong and moderately strong enhancements of H14 and 12 $\alpha,\beta$ , respectively, upon irradiation of H20 suggests that the 17 $\alpha$  side chain of the major conformer bears an extended geometry with a closer distance between H20 and H14 than between H20 and 12 $\alpha,\beta$ . This is only consistent with conformers **2b** and **2c**, which have distances between H20 and H14 of 2.0 and 2.2 Å and between H20 and 12 $\alpha$  of 2.1 and 2.5 Å, respectively. Comparing **2b** and **2c**, the weak enhancement of 16 $\alpha$  upon irradiation of H27 is consistent with the expected weak NOE intensity between H27 and 16 $\alpha$  of conformer **2c** but is inconsistent with the expected strong NOE intensity between H27 and 16 $\alpha$  of conformer **2b**. Conformer **2c** thus is considered the major conformer.

As for minor conformers, conformer **2d** can be ruled out as a contributing conformer because of the absence of an observable NOE between H27 and H14 or 15 $\alpha$ . For conformer **2f**, the expected weak enhancement of H14 upon irradiation of H20 suggests only a minor contribution since the observed enhancement is strong. The geometrically similar conformer, conformer **2e**, could not be ruled out with NOE data as a minor conformer. The presence of the syn orthogonal conformer **2a** is clear from the NOE enhancement of 12 $\alpha,\beta$  upon irradiation of H27. All other conformers of **2** have a distance between H27 and 12 $\alpha,\beta$  greater than 5 Å. The NOESY cross-peak between H21 and 12 $\alpha,\beta$  further supports the presence of conformer **2a** since all other predicted conformers bear a distance between H21 and 12 $\alpha,\beta$  greater than 5 Å.

The low-frequency region of the 2D NOESY spectrum of **3** displays additional cross-peaks not found in the similarly patterned 2D NOESY of **1** and **2** (Figure 8). Aside from the cross-peaks between H20 with 12 $\alpha,\beta$ , H14, and 16 $\alpha$  and H27 with 12 $\alpha,\beta$  and 16 $\alpha$  analogous to those observed for **1** and **2**, additional weak cross-peaks between H21 and H27 with an overlapping region consist-

ing of H14 and 15 $\alpha$  appear. Also, weak cross-peaks between the methylene protons of the 23-CH<sub>2</sub>OH group and 12 $\alpha,\beta$  and 16 $\alpha$  are observable. A selective 1D NOESY of H20 reveals strong enhancements of H14 and 12 $\alpha,\beta$  and weak enhancement of 16 $\alpha$  (Figure 4c). The 1D NOESY of H27 displays the expected weak enhancements of 16 $\alpha$  and the overlapped regions consisting of 12 $\alpha,\beta$  and H14,15 $\alpha$  (Figure 4d).

Comparing these observed enhancements with expected NOE intensities for predicted conformers of **3** indicates the presence of at least three conformers (see Table 9). The observed weak NOE enhancements of H21 with H14 and H27 with the overlapped region consisting of H14 and 15 $\alpha$  are only consistent with the two predicted anti orthogonal conformers **3e** and **3f**. All other conformers of **3** have a distance between these protons greater than 5 Å. Similarly, the observed weak NOE enhancements of H21 with 12 $\alpha,\beta$  and H27 with 12 $\alpha,\beta$  are only consistent with the two syn orthogonal conformers **3a** and **3c**. The very weak enhancement between the 23-CH<sub>2</sub>OH methylene protons and 12 $\alpha,\beta$  is only consistent with the predicted syn orthogonal/extended conformer **3g**.

As for the extended conformers, **3b** and **3d**, the strong NOE enhancements of 12 $\alpha,\beta$  and H14 upon irradiation of H20 would be consistent with their presence. However, these strong NOE enhancements could reasonably result from an averaged contribution of the syn orthogonal conformers **3a** and **3c**, the anti orthogonal conformers **3e** and **3f**, and the syn orthogonal/extended conformer **3g**. Thus, other reasonable interpretations of the NOE data are feasible. The remaining extended conformer, **3h**, cannot be ruled out with NOE data, but the expected strong enhancement of 16 $\alpha,\beta$  upon irradiation of the methylene protons of the 23-CH<sub>2</sub>OH group suggests only a minor contribution.

## Discussion

The NOE data indicate that **1–3** each exist in solution as an equilibrating mixture of conformers. Unlike **3**, both **1** and **2** show the dihedral C18–C17–C20–C21 restricted to a similar range of rotation. For **1** and **2**, the position of the 17 $\alpha$  side chain ranged from the syn orthogonal conformers **1a** and **2a** to the anti orthogonal/extended conformers **1c** and **2e**, whereas for **3**, the 17 $\alpha$  side chain ranged from the syn orthogonal conformers **3a/3c** to the anti orthogonal conformers **3e/3f**. In particular, the NOE data indicate that **1d** and **2d**, which are analogous to **3e/3f** in side chain position, are not populated. Although the 17 $\alpha$  side chain of **1** and **2** appears to have a similar range of rotation, the NOE data do suggest that the relative populations of the major conformers of **1** and **2** are slightly different. For **1**, the NOE data indicates that the major conformer **1c** bears an anti orthogonal/extended 17 $\alpha$  side chain, whereas for **2**, the major conformer **2c** has an extended 17 $\alpha$  side chain. As for minor conformers, the NOE data suggests that the syn orthogonal conformer **2a** is more abundant in solution for **2** than **1a** is for **1**. This conclusion is rationalized from the H21, 12 $\alpha,\beta$  cross-peak found only in the 2D NOESY of **2**.

The presence of the anti orthogonal conformers only found in **3** can be explained by stabilization experienced by **3e** and **3f** as a result of hydrogen bonding between the 17-OH and 23-CH<sub>2</sub>OH groups. For **3**, intramolecular hydrogen bonding is not predicted for any of the other conformers according to the MM3 calculations.

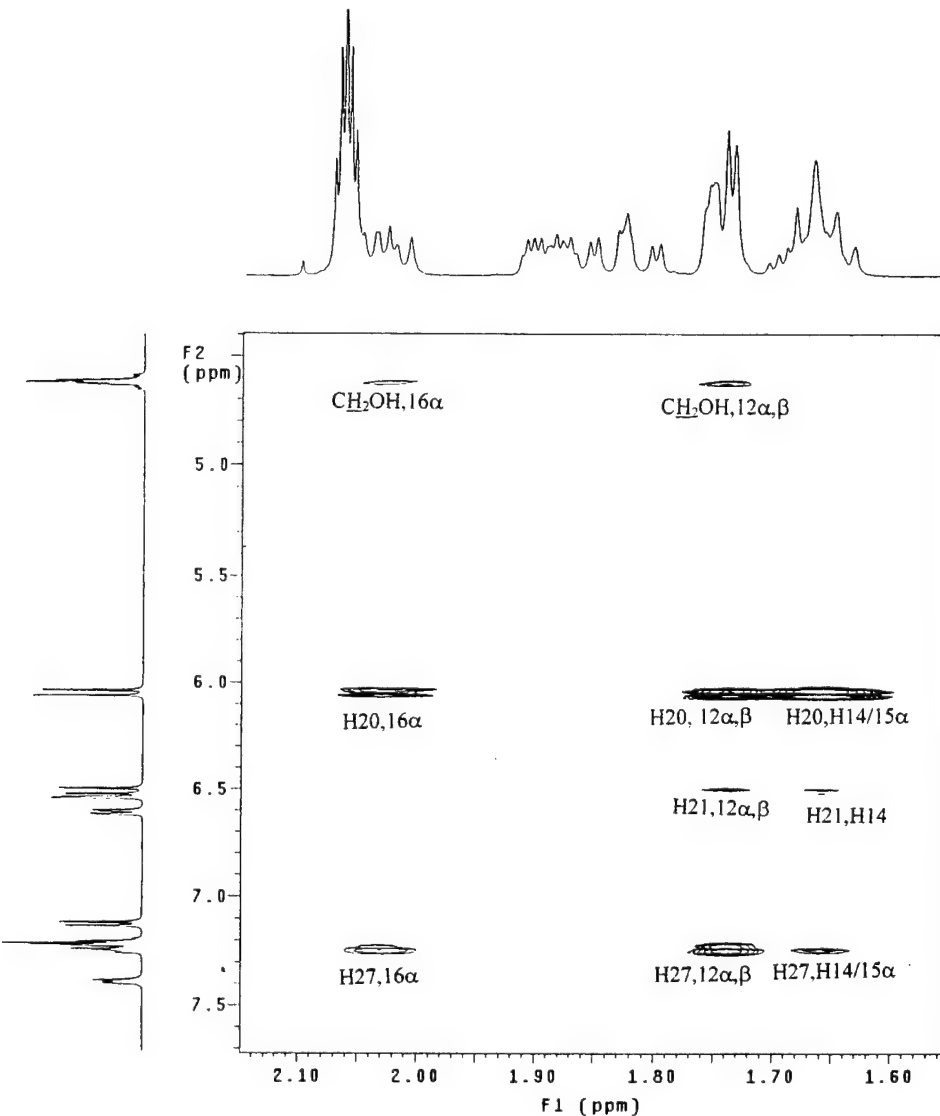


**Figure 8.** Spectral region of a 500 MHz 2D NOESY spectrum of **3** obtained with a mixing time of 500 ms. The NOE connectivities are indicated.

**Table 9. Summary and Comparison of Observed NOE Enhancements with Expected NOE Intensities<sup>a</sup> for Predicted Conformers of **3****

irradiated	enhanced	<b>3a</b>	<b>3b</b>	<b>3c</b>	<b>3d</b>	<b>3e</b>	<b>3f</b>	<b>3g</b>	<b>3h</b>	expt
H20	12α,β	w	s	w	s	s	s	s	s	s
H20	H14	s	s	s	s	w	w	s	s	s
H20	16α	s	w	s	w	w	w	s	w	w
H21	12α,β	w	n	w	n	n	n	n	n	w
H21	H14	n	n	n	n	w	w	n	n	w
H27	12α,β	s	n	s	n	n	n	n	n	w
H27	H14	n	n	n	n	w	w	n	n	w
H27	15α	n	n	n	n	w	w	n	n	w
H27	16α	n	s	n	s	w	w	w	n	w
CH <sub>2</sub> OH	12α,β	n	n	n	n	n	n	s	n	w
CH <sub>2</sub> OH	16α	w	n	w	n	w	w	n	s	w

<sup>a</sup> Expectations of strong (s), weak (w), and no (n) NOE enhancements correspond to H–H distances of 0–2.99, 3.0–4.99, and >5 Å.

The NOE data are mostly consistent with our statistical approach of evaluating contributing conformers from predicted <sup>13</sup>C shifts. The findings from multiple independent variable linear regression analysis of the <sup>13</sup>C data of **1** and **2**, that the major conformers **1c** and **2c** are 68% and 60% populated and that the minor conformers **1a** and **2a** are both 20% populated, are compatible with the

identities of major and minor conformers favored by NOE data. Additionally for **3**, a 36% populated syn orthogonal conformer **3a**, 34% populated extended conformer **3d**, 28% populated anti orthogonal conformer, and 2% populated syn/extended conformer **3g** is quite consistent with the NOE data.

Consistent with the NOE data, the statistical analysis suggests that conformers **1b**, **1e**, and **2d** are not found in solution. For **1**, although a 12% contribution of conformer **1d** is inconsistent with the NOE data, perhaps this is only a minor inconsistency since the identity of the major conformer and another minor conformer are consistent in the two methods. Furthermore, for **2**, a 20% population of conformer **2e** is consistent with the NOE data, although the NOE data do not clearly indicate that **2e** is the only additional minor conformer that is populated.

### Conclusions

This study reveals that the substituent on the phenyl group of the 17α,Z-phenylvinyl substituent of estradiols can affect the conformational equilibrium of the 17α side chain. Hydrogen bonding stabilization between the 17-

OH and a 23-CH<sub>2</sub>OH substituent of **3** results in an additional anti orthogonal conformer not found in **1** or **2**. The similarity in solution conformations of **1** and **2** suggests they occupy a similar receptor volume that is consistent with their similar RBA of 20 and 23 at the estrogen receptor. The different conformational equilibria of **3** may explain its significant RBA of 140, which is greater than estradiol itself. Other effects such as hydrogen bonding, size, and electronic effects of the substituents may also play roles. These results can be applied to the design of subsequent ligands which will examine these conformational and substituent effects.

## Experimental Section

HMQC, COSY, 1D and 2D NOESY spectra were obtained on a Varian Unity INOVA instrument at 500 MHz. DEPT and <sup>13</sup>C spectra were obtained on a Varian Mercury instrument at 300 MHz.

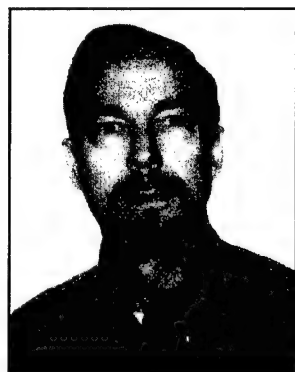
**Acknowledgment.** We thank Dr. Roger Kautz for valuable assistance concerning the NMR experiments. This work has been supported in part by PHS award (R01-CA-81049) and a grant from the U.S. Army (DAMD17-99-1-9333).

JO000806H

# Synthesis of Auger Electron-Emitting Radiopharmaceuticals

Robert N. Hanson\*

Department of Chemistry, Northeastern University, Boston, MA 02115 USA



**Abstract:** Targeted radiotherapy using Auger electron-emitting pharmaceuticals offers both advantages and challenges compared to alternative  $\alpha$ - or  $\beta$ -emitting agents. The low energy Auger electrons deposit their energy within the target cell thereby minimizing collateral damage. To achieve this effect, however, the radiopharmaceutical must incorporate the appropriate radionuclide, be efficiently synthesized, and once administered, be distributed selectively to its biological target. This review covers the synthesis of agents which have prepared over the past decade either as Auger electron-emitting radiopharmaceuticals or which have the potential as such. While not an exhaustive review, the major classes of agents, such as hormone receptor ligands, nucleoside analogs and intercalating agents are described.

## I. INTRODUCTION

Targeted radiotherapy, using internally emitted radiation, offers an alternative to the use of traditional radiation therapy or boron neutron capture therapy. The key features in this modality include the ability to direct the agent to the target tissue using a biological marker, the deposition of high linear energy transfer (LET) radiation at the site in a short period of time, and to have that energy transfer result in a localized cytotoxic event. The result of this process is to cause a high lethality rate among targeted populations of cells, often neoplastic cells, while generally sparing neighboring normal or nontargeted cells. Aspects of this process, e.g., use of antibodies and oligonucleotides to target cells, microdosimetry and the use of alpha-emitting radionuclides, are discussed in accompanying reviews in this issue.

Unlike  $\beta$ - or  $\alpha$ -emitting radionuclides, which deposit their LET effects over several cell diameters, the low energy Auger electrons emitted during radioactive decay deposit their energy within subcellular dimensions [1-3]. As a result, for a compound labeled with an Auger electron-emitting radionuclide to exert a cytotoxic effect, it has to be able to penetrate within the cell. In addition, for the agent to generate a lethal event, that localization should be within the proximity of the nuclear DNA. As described elsewhere, and previously reported,

cell death is associated most closely with the ability to cause double strand breaks in the DNA as a consequence of the shower of low energy electrons. Therefore, for an Auger electron-emitting radiopharmaceutical to have therapeutic potential, 1. a radionuclide must have an appropriate radiation decay profile, 2. a radionuclide should be able to be economically prepared in reasonably high specific activity and purity, 3. a radionuclide should be incorporated efficiently into a carrier molecule, 4. a carrier molecule should display biodistributional selectivity for the target tissue, and 5. in the target tissue, the agent should associate with the nuclear DNA complex for a time consistent with the half-life of the radionuclide. To date, virtually no Auger electron-emitting radiopharmaceutical has met all of these criteria. However, sufficient data both from *in vitro* studies with putative Auger emitters and from  $\alpha/\beta/\gamma$ -emitting radiopharmaceuticals suggest that success may be achieved with improved targeting mechanisms.

Based on the previously listed criteria, one is left with a relatively small set of available radionuclides with which to work (Table 1).

**Table 1. Auger Electron-Emitting Radionuclides for Use in Radiopharmaceutical Synthesis**

Chromium-51	Gallium-67	Bromine-77, 80m
Indium-111	Iodine-123, 125	Platinum-193m
Thallium-201		

\*Address correspondence to this author at the Department of Chemistry, Northeastern University, Boston, MA 02115 USA; Phone +1-617-373-3313; Fax: +1-617-373-8795; e-mail: ro.hanson@nunet.neu.edu

The most prominent of the Auger emitting radionuclides are the isotopes of iodine (I-125 and I-123) and bromine (Br-77 and 80 m). To a much less degree, studies have been reported related to the Auger effects of In-111 and Pt-193m. The other radionuclides that emit Auger electrons as part of their decay scheme, however, either have other emissions ( $\gamma$ ,  $\beta^+$ ,  $\beta^-$ ), half-life considerations or production characteristics that preclude their use as potential Auger-radiotherapeutics. The chemical properties of the radiohalogens allow them to be more readily incorporated into organic molecules by traditional synthetic methods, whereas the metal ions require chelation techniques [4,5]. These two strategies, as shown later, influence the types of targeting agents to which they are bound.

The low energy of the Auger electrons requires that they be emitted as close to the nucleus of the cell as possible to exert their lethal effect. Therefore, the carrier molecule for the radionuclide has to cross the cell membrane either by passive diffusion or via a specific carrier mediated process. Once inside the cell, the carrier-radionuclide complex has to bind selectively to the DNA or a DNA associated protein. This criterion dramatically reduces the number of potential carriers available for molecular manipulations (Table 2).

**Table 2. Mechanisms for Nuclear/Intracellular Localization**

1.	Nuclear Receptor Binding
2.	DNA-directed Agents
3.	Other Intracellular Targets

For the treatment of cancers with Auger emission radiotherapy, the most promising carrier molecules are the steroid hormones (via their receptors), DNA directed agents (nucleosides, intercalators, groove binding) and a few proteins and peptides [6]. Given the available radionuclides, there are relatively few options to exploit. This is in a distinct contrast to those  $\beta$ - or  $\alpha$ -emitting agents which do not require that degree of localization.

The primary objective of this review is to cover the progress since 1990 [7] in the preparation of radiotherapeutic agents bearing (potential) Auger electron-emitting radionuclides. Because the biophysical constraints imposed on this approach have limited its utility, a secondary objective will be to consider potential agents, based on work done with other radiodiagnostic or radiotherapeutic materials.

## II. HORMONE RECEPTOR LIGANDS

The mechanism of action of the steroid hormones has made the preparation of labeled analogs one of the major foci of radiopharmaceutical development. Receptors for the endogenous hormones are overexpressed in a number of human carcinoma cell lines. The circulatory steroids enter all cells by passive diffusion, however, only responsive cells contain the requisite hormone receptor. Binding of the hormone to its cognate receptor in the nucleus of the cell initiates a series of events which includes the binding of the steroid-receptor complexes to the nuclear DNA. The high affinity for the receptor, the selectivity of the hormone-receptor interactions, and the avidity of the complex for the DNA combine to provide the basis for radiotherapy using Auger electron-emitting steroid hormone receptor ligands [8]. Although success in achieving the affinity and selectivity for the estrogen receptor has been the greatest, synthesis of radiolabeled androgen and progestin receptor ligands have been reported in the past 10 years.

### A. Estrogen Receptor Ligands

During the 1980's the synthesis of a number of radiohalogenated analogs of estradiol were reported. The reviews by Katzenellenbogen [9] and Cummins [10] describe the labeling methods and biological properties of many of these ligands. While most of the emphasis was focused on the radiodiagnostic potential of these agents, the presence of Auger electrons from the decay of I-123/125 and Br-77/80 m initiated interest in their radiotherapeutic applications. The compounds that were most extensively evaluated were the  $16\alpha$ -halogenated (I/Br)-estradiols and the  $17\alpha$ -halo (I/Br) vinyl estradiols. The former were prepared by nucleophilic displacement of the appropriately substituted  $16\beta$ -X-estradiol. The latter were synthesized using the radiohaloestannylation methodology that we developed in the early 1980's. Both methods provided target compounds rapidly and in high yields (Fig. 1). Studies with these agents demonstrated that the presence of the halogen at either position was tolerated or, in the case of the  $17\alpha$ -halovinyl estrogens, beneficial to binding. Additional substituents at the  $11\beta$  or  $7\alpha$  positions also enhanced receptor binding. *In vitro* studies indicated that radiocytotoxicity was receptor mediated and, therefore, validated this approach.

More recent synthetic approaches have focused on two aspects, the enhancement of affinity within the estradiol structure, or identification of

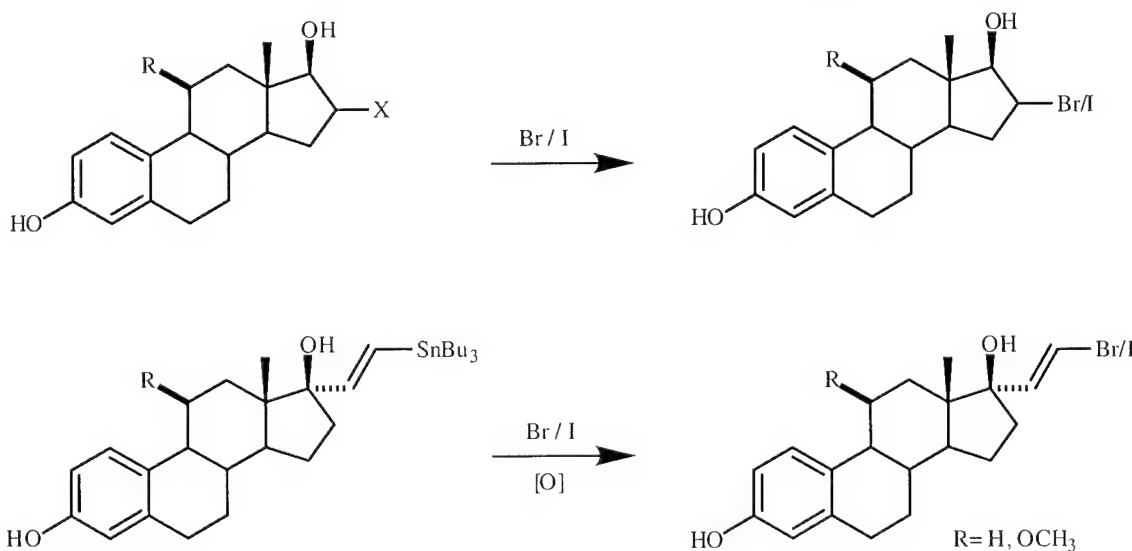


**Fig. (1).** Radiobromination/iodination of estradiols.

nonsteroidal estrogens with possibly better pharmacokinetic properties. Because both approaches utilized the destannylation methodology for introduction of the Auger emitting radiohalides, the challenges were primarily associated with the synthesis of the precursor trialkylvinylstannanes. Previous studies [11] had demonstrated that the 17 $\alpha$ -Z-halovinyl estradiols had higher affinity than the corresponding 17 $\alpha$ -E-isomers. Small lipophilic substituents at the 11 $\beta$ -position provided an additional enhancement of relative binding affinity (RBA) [12]. The synthesis of the 11 $\beta$ -vinyl/ethyl 17 $\alpha$ -Z-tributylstannylvinyl estradiol precursor for radiohalogen labeling is shown in Fig. 2. The process involved at least 13 steps with an overall yield of <2%, prior to the radiohalogenation (the E-

isomer can be obtained in ~4% overall yield). As a result, few of these analogs have been evaluated *in vitro* or *in vivo*. Initial data suggest that the radiocytotoxicity is retained, however, the physicochemical properties of the individual compounds produce variations in the pharmacokinetics. Additional work by Cummins [13] and Quincy [14] have also utilized the 17 $\alpha$ -iodovinyl group to prepare labeled estrogenic ligands, although with imaging as the objective.

The alternate approach for estrogen receptor ligands utilizes a nonsteroidal structure. DeSombre, *et al.* prepared the [Br-80m] labeled bis(hydroxyphenyl)ethylene [15]. While initially prepared via direct radiobromination of the

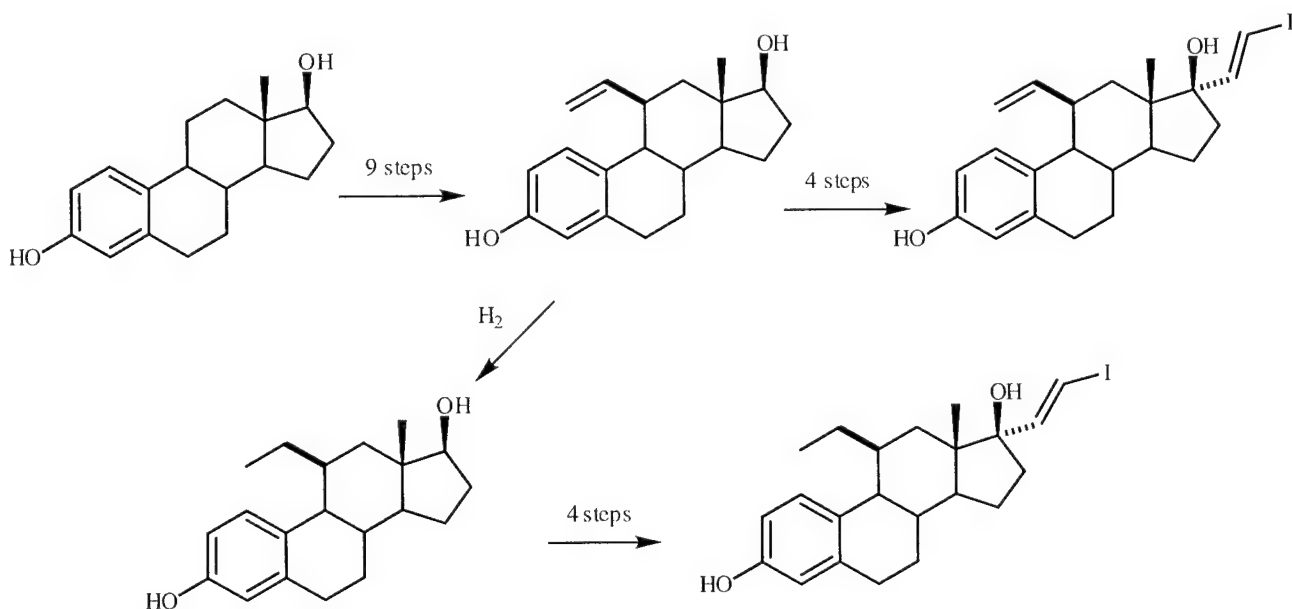


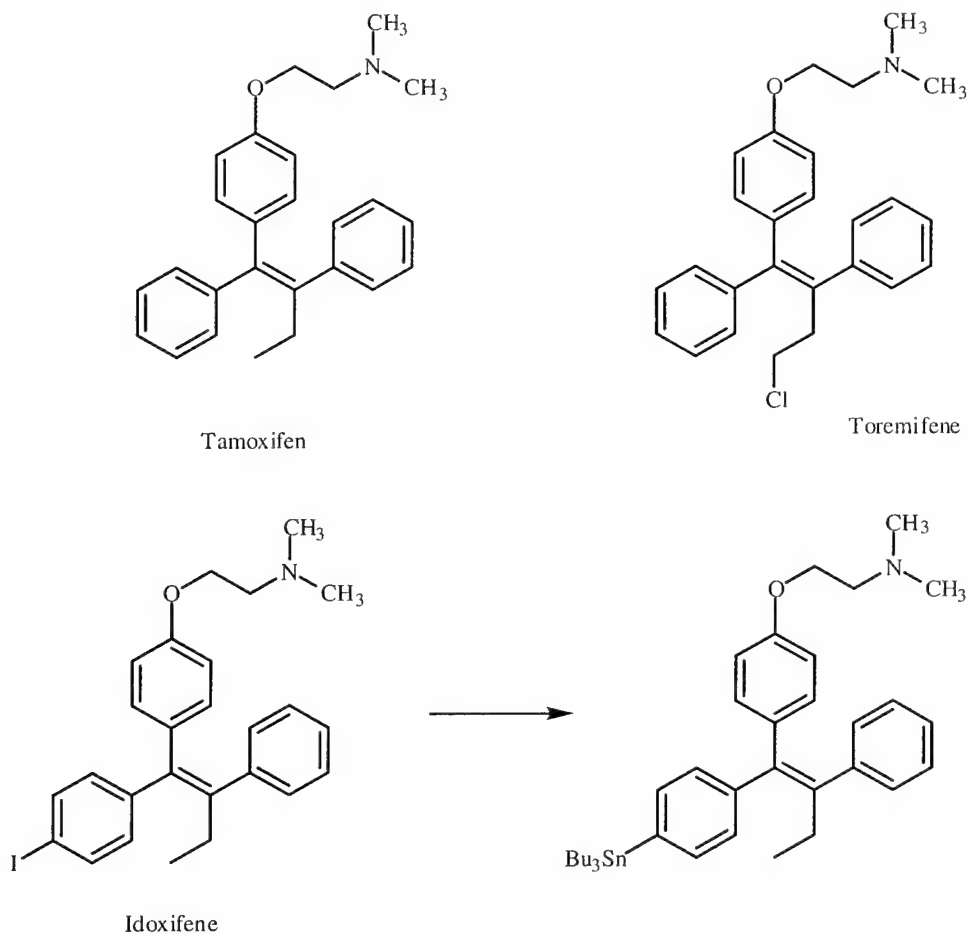
**Fig. (2).** Synthesis of 11 $\beta$ -substituted estradiols.

**Fig. (3).** Bis- and tris-hydroxy-triphenylethylene bromide.

protected material, better yields of purer product were obtained by using the destannylation methodology. Comparison with the 11 $\beta$ -substituted 17 $\alpha$ -iodovinyl estradiols suggested that some pharmacokinetic advantages were associated with the nonsteroidal structure. In order to improve receptor binding, an analog with an additional phenolic group has been prepared (Fig. 3). The initial synthesis of the stannylic intermediate was achieved using transmetallation of the vinyl bromide with alkyl lithium followed by quenching with trialkyltin halide, however, the yield in the final step was low. Use of hexabutylditin and

Pd(0)catalyst raised the yield by an order of magnitude. Biological studies with these labeled products (Br-80m/I-123) are currently undergoing *in vitro* evaluation.

An alternate approach to the use of labeled estrogenic agonists is the preparation of antagonists. Although both steroid and nonsteroidal antagonists have been described in the literature, only labeled derivatives of nonsteroidal antagonists have been reported. For example, idoxifene has been prepared and evaluated as a selective estrogen receptor modulator (SERM) and

**Fig. (4).** Nonsteroidal estrogen receptor ligands (antiestrogens).

its resynthesis with the addition step for replacement of iodine by tributyltin would provide the immediate precursor for labeling with either of the isotopes of iodine (Fig. 4).

## B. Progesterone Receptor Ligands

The design of radiolabeled progesterone receptor seeking ligands, as described by Brandes and Katzenellenbogen, has been hampered by several factors [16,17]. A major problem is that the endogenous ligand, progesterone, has a binding affinity for its receptor that is almost an order of magnitude less than that of estradiol for the estrogen receptor,  $4.5 \times 10^{-9}$ M vs.  $3 \times 10^{-10}$ M. As a consequence, a ligand receptor complex is less likely to remain associated with the nuclear DNA long enough for therapeutically relevant Auger emitting radionuclides to deposit their energy at the site. In addition, structure-activity studies on the progesterone receptor ligands provided relatively

ligands for the progesterone receptor [20]. Salman, *et al.* introduced the radiohalogen at the terminus of a  $17\alpha$ -haloalk-1-ynyl-19-nortestosterone in an attempt to enhance the affinity of the compound for the receptor [21]. While these compounds were chemically stable and relatively resistant to metabolism, they displayed little ability to localize in progesterone receptor rich tissue, to be retained there or exert any radiocytotoxic effect.

Since 1990, most of the efforts in the area have focused on the radiodiagnostic applications of the labeled progestins [22]. A number of the syntheses, however, employed labels that could be considered for radiotherapy given the appropriate radionuclide. Examples of these syntheses are shown in Fig. 6 and the putative radiosynthesis with the Auger emitting nuclide is provided. Van Lier's group synthesized the  $17\alpha$ -iodovinyl testosterone and 19-nortestosterone derivatives and evaluated their radioiodinated forms as ligands for the progesterone (and androgen) receptors [23]. Their

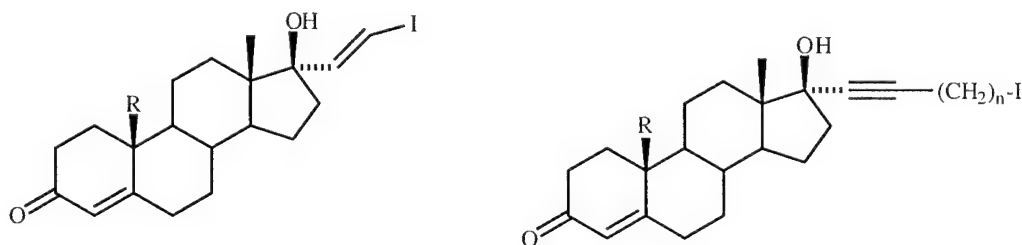


Fig. (5). Radiolabeled Derivatives of ethisterone and norethisterone.

few examples of compounds that had relative binding affinities (RBA) significantly greater than progesterone itself. Among that subset, even fewer were amenable to radiolabeling at sites that would be chemically or metabolically stable (Fig. 5). During the 1980's Hochberg, *et al.* described the preparation of the  $17\alpha$ -iodovinyl testosterone (ethisterone) and 19-nortestosterone (norethisterone) analogs in their radiolabeled form using the halodestannylation methodology [18,19]. The Schering group also explored these as potential

results essentially confirmed previous findings regarding the inadequacy of the ligands.

Based on the studies of Brandes and Katzenellenbogen which were primarily directed to F-18-labeled progesterone ligands, Van der Bos and Rijks prepared and evaluated a series of four iodinated progestins [24,25]. Two were the E- and Z-isomers of  $17\alpha$ -ido-19-nortestosterone previously evaluated, two were the E- and Z-isomers  $17\beta$ -hydroxy- $17\alpha$ -iodovinyl-11-

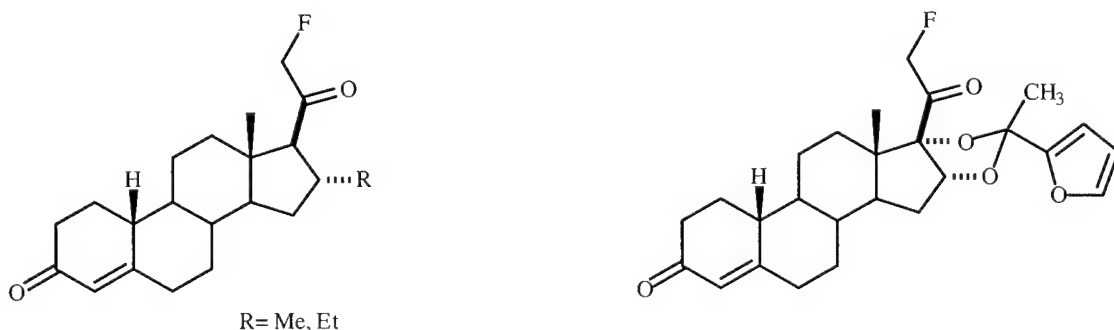


Fig. (6). Radiofluorinated progesterone receptor ligands.

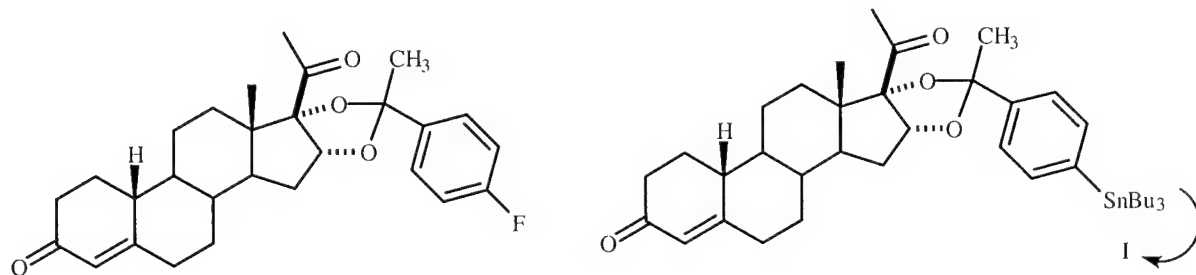


Fig. (7). Use of tributylstannyl analog as precursor for iodine radionuclide.

methylene-19-norgon-4-ene-3-one [ORG 3236 analogs], and the 21-iodophenoxy-16- $\alpha$ -ethyl-19-norpreg-4-ene-3,20-dione (ORG-2058 analog). The two ORG 3236 compounds had RBA values significantly greater than progesterone while the ORG 2058 analog bound with only 7% of the affinity of the endogenous ligand. Radiolabeling was achieved via the corresponding tributylstannyl precursor in good yields and high radiochemical purity. *In vivo* tissue distribution studies were disappointing for all of the ligands. Only the Z-isomer of the iodovinyl ORG-3236 analog possessed selectivity for the progesterone rich tissues in normal female rat. However, this selectivity was not observed in the induced mammary tumors.

Although the studies focused on imaging, the failure to be retained by the target tissues would also be of concern for radiotherapeutic applications as well.

Reevaluation of the work of Katzenellenbogen may provide additional possibilities for radioiodinated analogs of progesterone receptor ligands (Fig. 7). In particular the work with the 16 $\alpha$ , 17 $\alpha$ -dioxolanes provides opportunities to synthesize the corresponding iodinated analogs of the fluorinated compounds [26-28]. Conversion to the corresponding tributylstannyl derivatives followed by radioiododestannylation should yield target radiochemicals for *in vitro* and *in vivo* evaluation. Whether such products would overcome the deficiencies seen with previous agents, i.e., reduced affinity high nonspecific binding or metabolic lability, remains to be seen. A novel variation which would be amenable to the incorporation of a Auger-emitting metal ion has also been reported by this group [29].

### C. Androgen Receptor Ligands

Many of the same limitations imposed on progesterone receptor-directed ligands are encountered in the chemistry of the androgen

receptor targeted agents. The endogenous ligands, testosterone and 5 $\alpha$ -dihydrotestosterone have receptor affinities an order of magnitude less than that observed for estradiol at the target site. While there is an extensive literature related to androgenic and anabolic steroids, few of those compounds have higher affinities than 5 $\alpha$ -DHT for the target receptor. In addition, the endogenous ligands are rapidly metabolized to products with much lower receptor affinities. As a result, very few compounds have been described which have high affinity, metabolic stability and the potential for incorporation of a radionuclide possessing the desired properties.

The work with radiolabeled androgenic steroids over the past 10 years has concentrated primarily on their radiodiagnostic (PET and SPECT) potential. This mostly represented an extension of studies conducted during the late 1980's in which radiohalogens I-125 or F-18 were incorporated at the 7 $\alpha$ , 16 $\alpha$ , or 17 $\alpha$ -positions (Fig. 8) [30-33]. These early results were generally disappointing in that the radiochemicals exhibited either little specific binding or metabolic lability, or both. The challenges, therefore, were to improve the receptor affinity and the stability of the C-I bond.

Hochberg and co-workers extended their studies of the 17 $\alpha$ -[<sup>125</sup>I]-iodovinyl testosterone and nortestosterone radioligands with the preparation of E- and Z-17 $\alpha$ -iodovinyl-7 $\alpha$ -methyl nortestosterone. The E-isomer was twice as potent as the Z-isomer but still less than 5 $\alpha$ -DHT (RBA = 12 vs. 53, R1881 = 100 in rat cytosol). Unfortunately, when evaluated by Ali, *et al.*, the agent demonstrated little selectivity *in vivo* [23,34]. As a result, this compound was not examined for its ability to cause radiation induced cell death. Hochberg's group subsequently prepared a series of 7 $\alpha$ -ido (and fluoro) androgens as potential imaging agents. From this series, the radiohalogen was introduced by simple nucleophilic displacement into a steroid nucleus bearing appropriate 19/17 $\alpha$  substituents [35,36]. They evaluated the effects of dihydro testosterone vs. dihydro nortestosterone

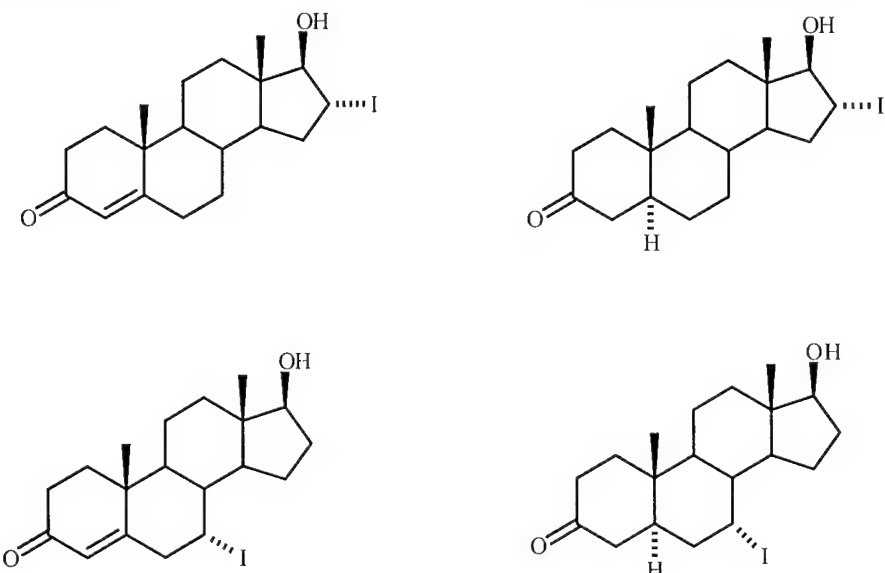


**Fig. (8).** radioiodinated (dihydro)testosterone derivatives.

vs. 17 $\alpha$ -methyl dihydro(nor)testosterone. While the affinities compared to 5 $\alpha$ -DHT were quite good (RBA = 25-123, DHT = 100) the radioiodinated agents were ineffective both *in vitro* and *in vivo*. As a result, no further work was pursued with those radiochemicals.

Radiolabeled antiandrogens constitute an even smaller series of potential therapeutic agents. This is due in part to the relatively small number of compounds that display this type of pharmacological activity. Until recently only flutamide, anandron and bicalutamide were the only

agents approved as antiandrogens although newer nonsteroidal compounds are in clinical trials. (Fig. 9). Miller and coworkers [37] reported the synthesis of radioiodinated bicalutamide via the triazene and trimethyltin intermediates. The iodinated derivative had affinity greater than the parent compound (3.1 nM vs. 11.0 nM), however, this was still poorer than testosterone (1.1 nM). In their I-125/123 labeled form this radiochemical may have potential as a radiotherapeutic agent, but no further data has been provided since the initial disclosures.

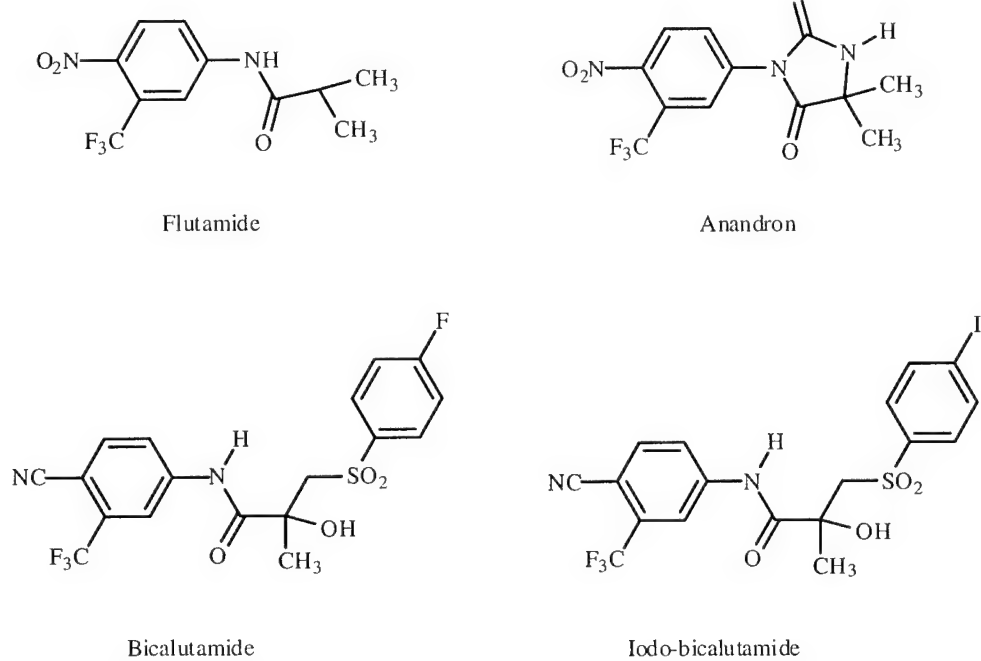


**Fig. (9).** Antiandrogens and radioiodinated analog.

## D. Summary

The past decade has seen advances in the synthesis of Auger-emitting ligands, both agonists and antagonists, for the steroid hormone receptors. Strategies have been developed for maintaining substantial affinity for the receptor and imparting metabolic stability in most cases. Use of the radioiododestannylation has been the most successful means for rapidly incorporating the radiohalogen in high specific activity. So far only the estrogen receptor-directed agents have demonstrated the ability to produce significant tumor cell killing. Successful extension to therapy remains to be shown for the estrogenic ligands. Improvements in receptor affinity and metabolic stability are required before the progesterone and androgen receptor directed agents can be evaluated as therapeutic agents.

## III. DNA DIRECTED AGENTS

This section examines the work done over the past 10 years to develop agents that directly target the DNA. Deoxyribonucleosides (D nucleotides)

and DNA intercalating agents constitute two other classes of compounds capable of imparting the cytotoxic effects of Auger-emitting radionuclides to the nuclear DNA. Labeled analogs of the deoxyribonucleotides can be incorporated into the DNA by the enzyme DNA polymerase if they resemble the endogenous substrate. This is one of the mechanisms by which antineoplastic drugs such as 6-mercaptopurine, 6-thioguanine, and adenine arabinoside, exert their cytotoxic effects. Appropriate nucleosides containing iodine or bromine could also be incorporated into the DNA and, upon disintegration, provide the low energy electron shower directly onto the DNA. Intercalating agents, on the other hand, are polycyclic compounds of either natural or synthetic origin that insert themselves between the bases of the DNA. Their ability to disrupt or to stabilize the structure of the DNA inhibits processes associated with DNA replication and ultimately exerts a cytotoxic effect. Auger-emitting analogs of the intercalating agents have the ability to induce strand breaks if the nuclear decay occurs during the time that the agent resides in the helix.

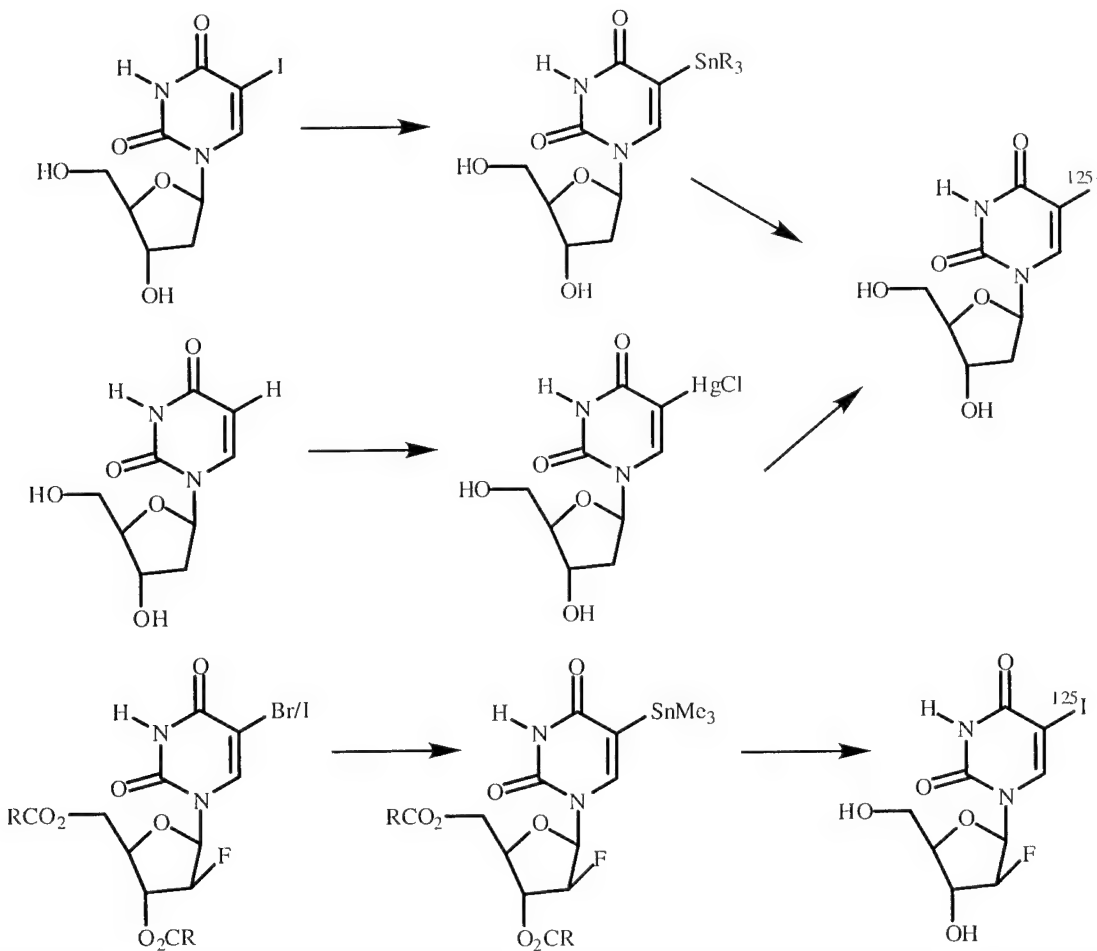


Fig. (10). representative syntheses of radioiodinated nucleosides.

## A. Radiolabeled Nucleoside Analogs

Among the nucleosides which could be applied to radiotherapy of tumors, halogenated analogs of uracil have been most extensively evaluated. This emphasis is the result of earlier studies that suggested that 5-iodouracil in particular is a close structural analog of thymidine and that it substitutes for the natural pyrimidine base in many of the ribosylation and kinase reactions preceding incorporation into DNA. The two major strategies are the synthesis of the radiohalogenated derivatives that incorporate improvements in the radiohalogenation procedure itself and the synthesis of nucleosides with improved biological characteristics.

Among the examples of radiohalogenations of nucleosides or their derivatives, two that best illustrate the methodological improvements are the synthesis of iododeoxyuridine and its 2-deoxy-2-fluoro analog (Fig. 10). The preparation of the former agent was reduced to a kit formulation by Foulon and Kassis [38,39]. In one method, they chloromercurated deoxyuridine to give the 5-chloromercuri-derivative which could be converted to the radioiodinated product using labeled iodide and Iodogen. The alternate procedure began with the cold iododeoxyuridine which was converted to the 5-triethylstannyl intermediate with Pd(0) catalyst and hexaalkylditin. Radioiodination with iodide and hydrogen peroxide then gave the desired product. Both methods were virtually instantaneous, however, the demercuration method

was more applicable to kit use. Vaidyanathan and Zalutsky [40] also employed the stannylation-destannylation method, however, their brominated or iodinated precursor required synthesis from the arabinoside and pyrimidine starting materials. The key iododestannylation step proceeded in greater than 85% yields to give the desired products.

The preparation of novel nucleosides/nucleotides is illustrated by two recent examples (Fig. 11). Dougan, *et al.*, [41] began with iododeoxyuridine and following protection as the 5-Fmoc ester coupled it at the 5-position of the pyrimidine with bis(tributylstannyl)ethylene. Activation at the 3-position of the sugar with a phosphoramidate group allowed the intermediate to be incorporated into an oligonucleotide that was ultimately radioiodinated using [I-125]-iodide and various oxidants. Reed, *et al.*, [42] also prepared a radioiodinated oligonucleotide via iododestannylation. In their synthesis, however, they utilized a sequence that contained a terminal hexamethyleneamine to which a 4-tributylstannylbenzoyl moiety could be conjugated. Radioiodination used their standard method and the product was obtained in good yields and high purity. Although the investigators implied potential radiotherapeutic applications, no data were provided.

## B. DNA Minor Groove Binding Agents

Another approach for the design of Auger-emitting DNA targeted agents involves labeling

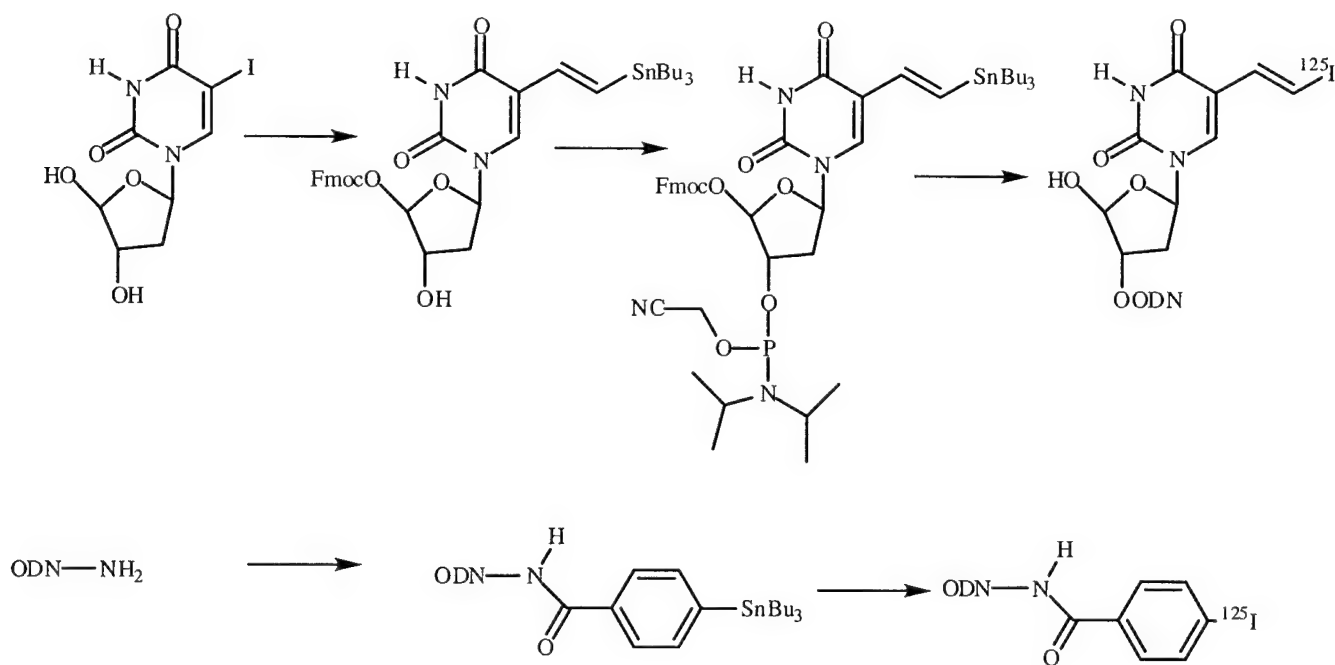
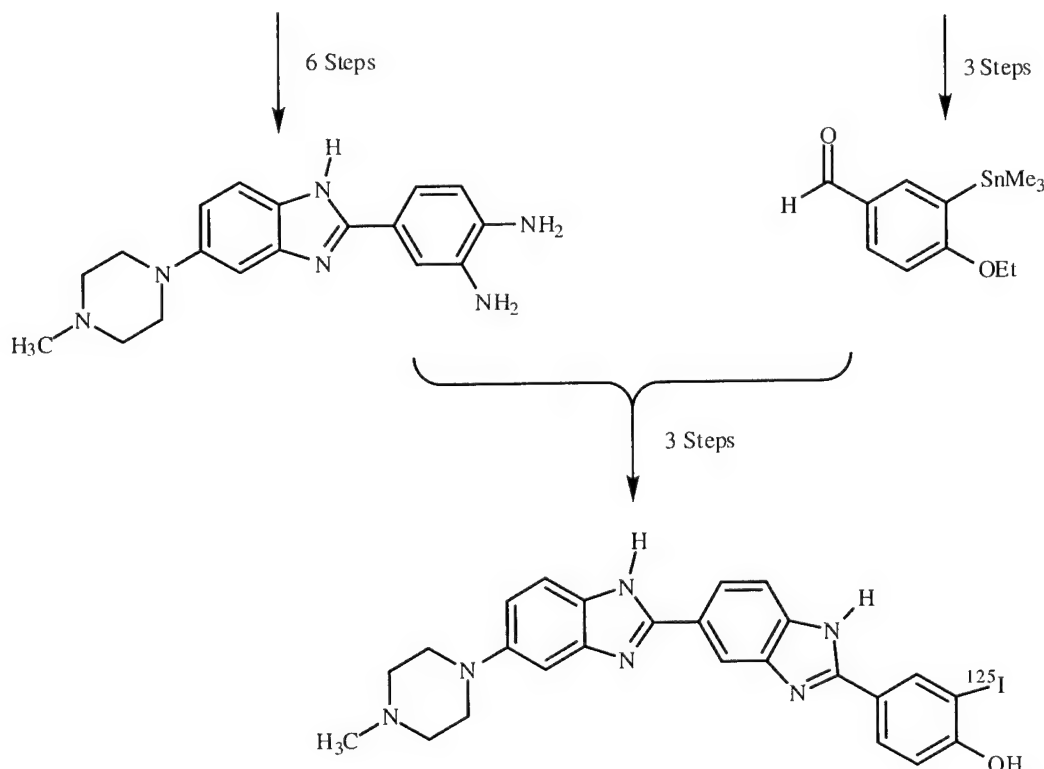


Fig. (11). Examples of Radioiodinated oligonucleotides.



**Fig. (12).** Synthesis of radioiodinated iodoHoechst 33342.

compounds that bind to the minor groove of the DNA via multiple hydrogen bonds. An example of the labeled intercalator method is illustrated by the synthesis and evaluation of [ $I$ -125]-iodoHoechst 33342 by Kassis and co-workers [43-46]. In their synthesis (Fig. 12), it was necessary to choose a site which could simultaneously permit the insertion of the trimethylstannyl group for radiolabeling while not adversely affecting the binding of the agent to the DNA. This was achieved by inserting an iodine on the distal aryl ring that could be replaced by the requisite stannyl moiety. With the availability of other sequence selective minor groove binding agents related to netropsin and distamycin [47] it should be possible to prepare and evaluate other Auger-emitting compounds as therapeutic agents. A relevant example is the modification of a sequence selective binder by Sigurdsson [48] to crosslink DNA. Replacement of the alkylating group by a labeled conjugate may achieve a comparable biological effect.

### C. Summary

In the area of DNA targeted agents there has been modest progress in the field of radiosynthesis. While methods have been developed for the efficient preparation of labeled nucleosides, both

for incorporation into DNA or into oligonucleotides that bind to the DNA, it is not clear whether the *in vivo* incorporation of the agents is sufficient to induce effective cytotoxicity. A similar problem may exist with the minor groove binding agents, however, the flexibility in their construction may ultimately lead to diagnostic or therapeutic agents.

### IV OTHER SYNTHESIS OF AUGER ELECTRON-EMITTING AGENTS

Although the majority of radiosynthesis of (potentially) Auger electron-emitting agents have focused on the nuclear DNA as their ultimate target, studies on other approaches have also been reported. Radioiodinated antibodies with anticancer potential continue to be evaluated, with the utilization of Auger electrons perhaps as part of their mechanism of action. While most radioiodinations use the conventional electrophilic incorporation with an oxidant [49,50], others use the trialkylstannylaryl carboxylate NHS ester conjugating agent [51]. This latter procedure continues to generate interest, not only for its diagnostic potential but also for incorporating Auger electron-emitting radionuclides [52-56]. Since there have been some studies exploring the utility of Auger emissions as a therapeutic adjunct

in the MIBG treatment of neuroblastoma [57,58] syntheses of other radiolabeled MIBG analogs have been reported [59]. Whether this is a viable approach to therapy remains to be seen. Lastly, the preparation of a somatostatin analog containing a chelated Auger electron-emitting radionuclide was described by Heppeler, *et al.* [60]. While little biological data were provided, its synthesis constituted one of the very few instances that did not employ a radiohalogen.

## NOTE ADDED IN PROOF

Since the submission of the review, three relevant manuscripts have been published. The first article involved the preparation and evaluation of new nonsteroidal antiandrogens related to bicalutamide ( Kirkovsky, *et al.*, *J. Med. Chem.* **2000**, *43*, 581-590). The second paper evaluated the binding of iodinated Hoechst 33258, a structural analog of the DNA intercalator prepared by Kassis (Squire, *et al.*, *Nucl. Acids Res.* **2000**, *28*, 1251-1258). The third paper described the production of In-114m, an Auger-emitting radionuclide, and the subsequent preparation of [In-114m]-DTPA-D-Phe-octreotide (*Nucl. Med. Biol.* **2000**, *27*, 183-188).

## ACKNOWLEDGMENTS

The author wishes to acknowledge the contributions over the past several years from Amin Kassis, S. James Adelstein and Eugene R. DeSombre whose understanding of the biological consequences of Auger emissions greatly exceeded his own. The author's research in the steroid field in general and radiolabeled estrogens in particular has been supported by awards from the Public Health Service (1RO1 CA81049), the Department of Defense (DAMD179919333), and the Department of Energy (DEFG0299ER62793).

## REFERENCES

- [1] Wheldon, T.E.; O'Donoghue, J.A. *Int. J. Radiat. Biol.* **1990**, *58*, 1-21.
- [2] Szumiel, I. *Int. J. Radiat. Biol.* **1994**, *66*, 28-341.
- [3] Volkert, W.A.; Hoffman, T.J. *Chem. Rev.* **1999**, *99*, 2269-2292.
- [4] Schubiger, P.A.; Alberto, R.; Smith, A. *Bioconj. Chem.* **1996**, *7*, 165-179.
- [5] Heeg, M.J.; Jurisson, S.S. *Acc. Chem. Res.* **1999**, *32*, 1053-1060.
- [6] O'Donoghue, J.A. *J. Nucl. Med.* **1996**, *37*, (Supp.) 35-65.
- [7] Howell, R.W.; Narra, V.R.; Sastry, K.S.R.; Rao, D.V. eds., "Biophysical Aspects of Auger Processes," American Institute of Physics, Woodbury, NY, **1991**.
- [8] DeSombre, E.R.; Hughes, A.; Gatley, S.J.; Schwartz, J.C.; Harper, P.U. In "Molecular Endocrinology and Steroid Hormone Action". Alan R. Lios, Inc. **1990**, pp. 295-309.
- [9] Katzenellenbogen, J.A. In "Estrogens, Progestins and Their Antagonists. Volume I," Pavlik, E.J. ed., Birkhauser, Boston **1996**, , pp. 197-242.
- [10] Cummins, C.H. *Steroids* **1993**, *58*, 245-259.
- [11] Napolitano, E.; Fiaschi, R.; Hanson, R.N. *J. Med. Chem.* **1991**, *34*, 2754-2759.
- [12] Hanson, R.N.; Napolitano, E.; Fiaschi, R. *J. Med. Chem.* **1998**, *41*, 4686-4692.
- [13] Cummins, C.H. *Steroids* **1994**, *59*, 590-596.
- [14] Quivy, J.; Leclercq, G.; Deblaton, M.; Henrot, P.; Velings, N.; Norberg, B.; Evrard, G.; Zeicher, M. *J. Steroid Biochem. Molec. Biol.* **1996**, *59*, 103-117.
- [15] DeSombre, E.R.; Mease, R.C.; Hughes, A.; Harper, P.U.; De Jesus, O.T.; Friedman, A.M. *Cancer Res.* **1988**, *48*, 899-906.
- [16] Brandes, S.J.; Katzenellenbogen, J.A. *Nucl. Med. Biol.* **1988**, *15*, 53-67.
- [17] Brandes, S.J.; Katzenellenbogen, J.A. *Mol. Pharmacol.* **1987**, *32*, 391-403.
- [18] Hoyte, R.M.; Rosner, W.; Johnson, I.S.; Zielinski, J.; Hochberg, R.B. *J. Med. Chem.* **1985**, *28*, 1695-1699.
- [19] Hochberg, R.B.; Hoyte, R.M.; Rosner, W. *Endocrinology* **1985**, *117*, 2550-2552.
- [20] Hofmeister, H.; Laurent, H.; Schalze, P.-E.; Weichert, R. *Tetrahedron* **1986**, *42*, 3575-3578.
- [21] Salman, M.; Stotter, P.L.; Chamness, G.C. *J. Steroid Biochem.* **1989**, *33*, 25-31.
- [22] Carlson, K.E.; Brandes, S.J.; Pomper, M.G.; Katzenellenbogen, J.A. *Nucl. Med. Biol.* **1988**, *15*, 403-408.
- [23] Ali, H.; Rousseau, J.; Van Lier, J.E. *J. Steroid Biochem. Molec. Biol.* **1994**, *49*, 15-29.
- [24] Van der Bos, J.C.; Rijks, L.J.M.; van Doremale, P.A.P.M.; de Bruin, K.; Janssen, A.G.M.; van Royen, E.A. *Nucl. Med. Biol.* **1998**, *25*, 781-789.
- [25] Rijks, L.J.M.; van der Bos, J.C.; van Doremale, P.A.P.M.; Boer, G.J.; de Bruin, K.; Janssen, A.G.M.; van Royen, E.A. *Nucl. Med. Biol.* **1998**, *25*, 791-798.

[26] Kym, P.R.; Carlson, K.E.; Katzenellenbogen, J.A. *J. Med. Chem.* **1993**, *36*, 1111-1119.

[27] Kochanny, M.J.; Van Brocklin, H.F.; Kym, P.R.; Carlson, K.E.; O'Neil, J.P.; Bonasera, T.A.; Welch, M.J.; Katzenellenbogen, J.A. *J. Med. Chem.* **1993**, *36*, 1120-1127.

[28] Bockman, B.O.; Bonasera, T.A.; Kirschbaum, K.S.; Welch, M.J.; Katzenellenbogen, J.A. *J. Med. Chem.* **1995**, *38*, 328-337.

[29] Wirst, F.; Skaddan, M.B.; Leibnitz, P.; Spies, H.; Katzenellenbogen, J.A.; Johannsen, B. *Bioorg. Med. Chem. Lett.* **1999**, *7*, 1827-1835.

[30] Hoyte, R.M.; Rosner, W.; Hochberg, R.B. *J. Steroid Biochem.* 1982, *16*, 621-628; *Biochem.* **1982**, *16*, 621-628.

[31] Symes, E.K.; Coulson, W.-F.; Farrant, R.D.; Milroy, E.J.G. *Biochem. Pharmacol.* **1985**, *34*, 317303178.

[32] Hoyte, R.M.; MacLusky, N.J.; Hochberg, R.B. *J. Steroid Biochem.* **1990**, *36*, 125-132.

[33] Hoyte, R.M.; Borderon, K.; Bryson, K.; Allen, R.; Hochberg, R.B.; Brown, T.J. *J. Med. Chem.* **1994**, *37*, 1224-1230.

[34] Hoyte, R.M.; Brown, T.J.; MacLuskey; Hochberg, R.B. *Steroids* **1993**, *58*, 13-23.

[35] Larabee, D.C.; Brown, T.J.; Hoyte, R.M.; Hochberg, R.B. *J. Nucl. Med.* **1997**, *38*, 402-409.

[36] Larabee, D.C.; Hoyte, R.M.; Nazareth, L.V.; Weigel, N.L.; Hochberg, R.B. *J. Med. Chem.* **1999**, *42*, 2021-2034.

[37] Kirkovsky, L.; Mukherjee, A.; Dalton, J.T.; Miller, D.D. [I-125]-Radioiodinated analogs as potential imaging agents for prostate cancer. 214<sup>th</sup> ACS National Meeting, Las Vegas, NV.

[38] Foulon, C.F.; Adelstein, S.J.; Kassis, A.I. *J. Nucl. Med.* **1996**, *37* (Supp.), 15-35.

[39] Kassis, A.I.; Adelstein, S.J.; Mariani, G. *Quant. J. Nucl. Med.* **1996**, *40*, 301-319.

[40] Vaidyanathan, G.; Zalutsky, M.R. *Nucl. Med. Biol.* **1998**, *25*, 487-496.

[41] Dougan, H.; Hobbs, J.B.; Weitz, J.I.; Lyster, D.M. *Nucl. Acids Res.* **1997**, *25*, 2897-2901.

[42] Reed, M.W.; Panyutin, I.G.; Hamlin, D. Lucas, D.D.; Wilbur, D.S. *Bioconj. Chem.* **1997**, *8*, 238-243.

[43] Harapanhalli, R.S.; McLaughlin, L.W.; Howell, R.W.; Rao, D.V.; Adelslein, S.J.; Kassis, A.I. *J. Med. Chem.* **1996**, *39*, 4804-4809.

[44] Kassis, A.I.; Harapanhalli, R.S.; Adelstein, S.J. *Radiat. Res.* **1999**, *152*, 530-538.

[45] Kassis, A.I., Harapanhalli, R.S.; Adelstein, S.J. *Radiat. Res.* **1999**, *151*, 167-176.

[46] Walicka, M.A.; Ding, Y.; Roy, A.M.; Harapanhalli, R.S.; Adelstein, S.J.; Kassis, A.I. *Int. J. Radiat. Biol.* **1999**, *75*, 1579-1587.

[47] Bailly, C.; Chaires, J.B. *Bioconj. Chem.* **1998**, *9*, 513-53.

[48] Sigurdsson, S.Th.; Hopkins, P.B. *Tetrahedron* **1994**, *50*, 12065-12084.

[49] Daghighian, F.; Barendswaard, E.; West, S.; Humm, J.; Scott, A.; Wielingham, M.C.; McGuffie, E.; Old, L.J.; Larson, S.M. *J. Nucl. Med.* **1996**, *37*, 1052-1057.

[50] Harapanhalli, R.S.; Matalka, K.Z.; Jones, P.L.; Mahmood, A.; Adelstein, S.J.; Kassis, A.I. *Nucl. Med. Biol.* **1998**, *25*, 267-278.

[51] Zalutsky, M.R.; Xu, F.J.; Foulon, C.F.; Zhao, X.-G.; Slade, S.K.; Affleck, D.J.; Bast, R.C., Jr. *Nucl. Med. Biol.* **1999**, *26*, 781-790.

[52] Wilbur, D.S.; Hamlin, D.K.; Srivastava, R.R.; Burns, H.D. *Bioconj. Chem.* **1993**, *4*, 574-580.

[53] Foulon, C.F.; Adelstein, S.J.; Kassis, A.I. *Bioorg. Med. Chem. Lett.* **1996**, *6*, 779-784.

[54] Yngve, U.; Hedberg, E.; Lovqvist, A.; Tolmachev, V.; Langstrom, B. *Acta Chem. Scand.* **1999**, *53*, 508-512.

[55] Vaidyanathan, G.; Affleck, D.J.; Zalutsky, M.R. *Bioconj. Chem.* **1998**, *8*, 724-729.

[56] Lindegren, S.; Skarnemark, G.; Jacobsson, L.; Karlsson, B. *Nucl. Med. Biol.* **1998**, *25*, 659-665.

[57] Mairs, R.J. *Eur. J. Cancer* **1999**, *35*, 1171-1173.

[58] Meco, D.; Lasorella, A.; Riccardi, A.; Servidei, T.; Mastrangelo, R.; Riccardi, R. *Eur. J. Cancer* **1999**, *35*, 1227-1234.

[59] Vaidyanathan, G.; Zalutsky, M.R.; DeGrado, T.R. *Bioconj. Chem.* **1998**, *9*, 758-764.

[60] Heppeler, A.; Froidevaux, S.; Macke, H.R.; Jermann, E.; Behe, M.; Powell, P.; Hennig, M. *Chem. Eur. J.* **1999**, *5*, 1974-1981.

## Conformational Studies of Novel Estrogen Receptor Ligands by 1D and 2D NMR Spectroscopy and Computational Methods

Albert B. Sebag, Robert N. Hanson\*, David A. Forsyth, Choon Young Lee

*Departments of Pharmaceutical Science and Chemistry, Northeastern University, 360 Huntington Avenue, Boston, MA 02115*

**Abstract:** The solution conformations of the novel estrogen receptor ligands, (17 $\alpha$ , 20E)-(p- $\alpha$ ,  $\alpha$ ,  $\alpha$ -trifluoromethylphenyl)vinyl estradiol (**1**) and (17 $\alpha$ , 20E)-(o- $\alpha$ ,  $\alpha$ ,  $\alpha$ -trifluoromethylphenyl)vinyl estradiol (**2**) were investigated in 2D and 1D NOESY studies and by comparison of  $^{13}\text{C}$  NMR chemical shifts with theoretical shieldings. The  $^1\text{H}$  and  $^{13}\text{C}$  assignments of **1** and **2** were determined by DEPT, COSY, and HMQC experiments. The conformations of the 17 $\alpha$ -phenylvinyl substituents of **1** and **2** are of interest because of their differing receptor binding affinities and effects in MCF-7 cell proliferation assays. A statistical method of evaluating contributing conformers of **1** and **2** from predicted  $^{13}\text{C}$  shifts of possible structures correlated quite well with conformational conclusions derived from the NOE data. The 17 $\alpha$  substituents of **1** and **2** apparently have a similar conformational preference in solution, suggesting that **1** and **2** could occupy a similar receptor volume.

## Introduction

As part of our efforts to develop more effective therapeutic agents for the treatment of breast cancer, we undertook the designing of (17 $\alpha$ , 20E)-(X-phenyl)vinyl estradiol compounds that can potently and selectively block the interaction of estradiol with its target receptor to impart the desired biological effect. In MCF-7 cell proliferation assay studies, we observed that (17 $\alpha$ , 20E)-(p- $\alpha$ ,  $\alpha$ ,  $\alpha$ -trifluoromethylphenyl)vinyl estradiol (**1**) antagonizes estradiol stimulation and is a very weak agonist with a relative binding affinity (RBA) of 7, compared to the native ligand estradiol at 100.<sup>1</sup> In contrast, under the same assay conditions, (17 $\alpha$ , 20E)-(o- $\alpha$ ,  $\alpha$ ,  $\alpha$ -trifluoromethylphenyl)vinyl estradiol (**2**) was a full agonist with an RBA of 71. We examine here whether *ortho* vs. *para* placement of the substituent in these *E*-isomers could produce a difference between the preferred conformations of **1** and **2** that could account for their distinguishable biological responses and varying binding affinity. In particular, if the conformational preferences differ and that difference were to be preserved upon binding to the receptor, it could affect the conformational mobility of the key helix-12 of the ligand binding domain (LBD) of the estrogen receptor (ER).<sup>2</sup>

Recently we showed that the placement of a substituent in the *ortho* or *para* position in some *Z*-isomers, i.e., (17 $\alpha$ , 20Z)-phenylvinyl estradiols did affect the conformational equilibrium of the 17 $\alpha$  side chain.<sup>3</sup> In that study, (17 $\alpha$ , 20Z)-(p-methoxyphenyl)vinyl estradiol and (17 $\alpha$ , 20Z)-(o- $\alpha$ ,  $\alpha$ ,  $\alpha$ -trifluoromethylphenyl)vinyl estradiol were found to exist in similar conformational equilibria which suggested they would likely occupy a similar receptor volume. These results were consistent with their similar RBA values of 20 and 23. In contrast, (17 $\alpha$ , 20Z)-(o-hydroxymethylphenyl)vinyl

estradiol, which had an RBA of 140, was found to exist in a different conformational equilibrium in terms of the distribution of structures varying in the angles of rotation about the bonds to the vinyl group. These results suggested that, in addition to position and electronic effects of the substituent, the preferred conformations of the  $17\alpha$  substituent of Z-compounds might account for some variation of the RBA values.

In this report, we present a conformational study of the 20E-isomers, **1** and **2**, using NMR and computational methods, to determine whether differences in the preferred conformation of **1** and **2** might also account for their distinguishable biological responses and binding affinities.

The key conformational feature to establish for **1** and **2** is the orientation of the  $17\alpha$  substituent relative to the steroid skeleton. In this study, we use molecular mechanics calculations to generate a set of possible conformations. Two types of NMR data are used in conjunction with the predicted conformations to evaluate which conformations are populated in solution. One approach is to use  $^{13}\text{C}$  chemical shifts in a comparison with shifts predicted for each of the geometries generated from the molecular mechanics calculations. The predicted  $^{13}\text{C}$  shifts come from empirically scaled GIAO (gauge including atomic orbitals) shielding calculations.<sup>4</sup> The other approach is to compare  $^1\text{H}$ - $^1\text{H}$  nuclear Overhauser effects established in one- and two-dimensional experiments, 1D and 2D NOESY, with predicted interatomic distances.

## Experimental

The syntheses and biological data of compounds **1** and **2** have been described elsewhere.<sup>5</sup>  $^1\text{H}$  NMR data were recorded at 25 °C for 5-8 mg samples dissolved in acetone- $d_6$  in 5 mm NMR tubes using a Varian Unity 500 MHz NMR spectrometer

equipped with a 5 mm Varian inverse probe. DEPT and  $^{13}\text{C}$  experiments were obtained on a Varian Mercury instrument at 75 MHz.

$^1\text{H}$  spectra were obtained with a spectral width (SW) of 8 kHz, a  $67^\circ$  pulse flip angle, a 1.7 s acquisition time (AT), a 2 s relaxation delay (RD) and digitized with 32768 points giving a digital resolution (DR) of 0.488 Hz per point. Chemical shifts were referenced to the residual  $^1\text{H}$  signal of acetone- $d_6$ .

$^1\text{H}$ -decoupled  $^{13}\text{C}$  spectra were recorded with a 18856 Hz SW, a  $60^\circ$  pulse flip angle, a 2 s RD and digitized into 65536 points to give a digital resolution of 0.575 Hz per point.

HMQC<sup>6</sup> experiments for single bond  $^1\text{H}$ ,  $^{13}\text{C}$  chemical shift correlation spectra utilized the BIRD sequence to suppress unwanted signals and GARP<sup>7</sup>  $^{13}\text{C}$  decoupling. Two sets of 256 time increments were obtained in the phase-sensitive mode with 32 transients obtained per time increment and a 2 s RD. The final matrix was processed with Gaussian functions.

COSY45<sup>8</sup> experiments were performed with 8 scans for each of 200 increments in  $\text{F}_1$ , 2048 data points in  $\text{F}_2$  and a relaxation delay of 2.0 s. The final matrix was symmetrized and processed with sine-bell exponential multiplication.

NOESY<sup>9</sup> experiments were performed with 32 scans for each of 256  $\text{F}_1$  increments, 2048 data points in  $\text{F}_2$ , with a relaxation delay of 2.0 s and a mixing time of 0.500 s. The final matrix was not symmetrized, but was processed with Gaussian weighing functions.

1D NOESY<sup>10</sup> spectra were obtained using a spectral width of 5000 Hz and 20500 points giving a digital resolution of 0.490 Hz per point, a mixing time of 0.500 s, a RD of

2.0 s, and a AT of 1.7 s. A Gaussian shaped pulse was used for selective irradiation.

## RESULTS AND DISCUSSION

### <sup>1</sup>H and <sup>13</sup>C Assignments

The <sup>1</sup>H NMR spectra of **1** and **2** in acetone-*d*<sub>6</sub> (Figures 1(a) and 2(a)) exhibit very little chemical shift dispersion in the low frequency spectral regions (1.2-2.5 ppm), precluding straightforward <sup>1</sup>H assignment even at 500 MHz. However, <sup>1</sup>H signals were assigned via application of HMQC and COSY techniques. The first step was to make <sup>13</sup>C shift assignments, based on our earlier studies of several 17 $\alpha$ -substituted estradiols,<sup>3</sup> DEPT experiments, and theoretical shielding calculations (see below). Then, geminal proton resonances were identified and all proton signals were correlated with directly attached carbons via an HMQC experiment. COSY experiments confirmed the initial assignments made by the HMQC experiment but did not, of course, distinguish between  $\alpha$  and  $\beta$  hydrogens in a given methylene group. This distinction was readily achieved by 1D NOESY experiments (Figure 1(b) and 2(b)). Using a Gaussian pulse, selective irradiation of the protons of the methyl group enhances protons on the  $\beta$  face of the C and D rings, viz., 11 $\beta$ , 12 $\beta$ , 15 $\beta$ , 16 $\beta$ , and H8. Table 1 lists the complete assignments of the <sup>1</sup>H and <sup>13</sup>C signals of **1** and **2**.

### Theoretical Carbon Chemical Shifts and Conformational Determination

The predicted low energy conformers of **1** and **2** (Figures 3 and 4) were generated using the MM3<sup>11</sup> force field through conformational searching by a previously described method.<sup>3</sup> The key dihedral angles are listed in Table 2 for the lowest energy conformers,

**1a-1c** and **2a-2h**, with energies within 1.6 kcal of the lowest energy conformers for **1** and **2**, respectively.

As the MM3 calculations show, significant changes in the  $17\alpha$  side chain conformation result in only minor energy differences. Most of the low energy conformers are within 1 kcal of the lowest energy conformer, making any conformational determination based purely on MM3 energy predictions unreliable. In MMX<sup>12</sup> and MM3 force fields, driving the dihedral angle C21-C20-C17-C13 shows a very shallow energy surface from  $85^\circ$  to  $165^\circ$ . In this region, discrete changes in the orientation of the phenyl to the vinyl group yielded numerous minima using either MM3 or MMX. Conformers **1a** and **1c** were kept as minima since they represent the upper and lower dihedral range of this shallow surface.

Conclusions regarding the preferred  $17\alpha$  side chain conformation of **1** and **2** were approached by applying a statistical method of determining contributing conformers from predicted  $^{13}\text{C}$  chemical shifts,  $\delta_{\text{pred}}$ , of MM3 determined conformers.<sup>3,13</sup> The  $\delta_{\text{pred}}$  were calculated for each MM3-predicted conformer by empirically scaling GIAO-calculated absolute shieldings,  $\sigma$ , obtained at the B3LYP/3-21G level with heteroatoms augmented at the 6-31+G\* level.<sup>4</sup> All shielding calculations were carried out with the Gaussian98 program.<sup>14</sup> Tables 3 and 4 list the  $\delta_{\text{pred}}$  of each MM3 conformer and the assigned experimental  $^{13}\text{C}$  chemical shifts,  $\delta_{\text{exp}}$ .

In this statistical method, the predicted  $^{13}\text{C}$  shifts of the C and D rings of all MM3 conformers of **1** and **2** were in each separate case treated as independent variables in a multiple independent variable regression analysis of the corresponding experimental data.<sup>15</sup>

The predicted  $^{13}\text{C}$  shifts of the A and B rings of all reasonable conformers of **1** and **2** were not used in this statistical analysis since all remain the same within 0.5 ppm regardless of the conformer. In contrast, while the shift differences are still relatively small,<sup>4</sup> most carbons in the C and D rings of **1** and **2** display larger than 1 ppm shift differences depending on the geometry. The regression analysis yielded fractional populations as the fitting parameters. All standard errors and confidence levels of the regression analysis were estimated using the Bootstrapping method.<sup>16</sup>

The results and corresponding estimates of uncertainties (standard errors) are listed in Table 5. Both **1** and **2** were found to have a major conformer, **1b**,  $72 \pm 32\%$ , and **2e**,  $65 \pm 33\%$ . Minor conformers are also indicated for each: **1a**,  $13 \pm 29\%$ , and **1c**,  $15 \pm 28\%$ ; and **2c**,  $33 \pm 18\%$ , and **2h**,  $2 \pm 22\%$ . It is important to note that the large corresponding standard errors make conclusions on the presence of minor conformers unreliable.

The success of this statistical approach for deducing percentage populations of participating conformations in fast exchange depends upon several conditions. Obviously, the molecular mechanics calculations must correctly identify all the possible contributing conformations and represent their conformations appropriately. The chemical shift calculations must also be reasonably accurate; confidence in this regard is engendered by the close match of predicted chemical shifts to experimental shifts at the positions that do not have conformationally dependent shifts. Finally, there must be substantial differences in chemical shifts among the possible conformations and unique combinations of chemical shifts for each. The large uncertainties in the statistical analyses of **1** and **2** shown in Table

5 arise from the relatively small differences in predicted shifts among the different conformers. The largest variations in the C and D rings are predicted to occur at C16 and C14. Thus, in this case it is sensible to take the statistical results only as a qualitative indicator of the major conformers rather than as a meaningful population analysis.

## NOESY Studies

The solution state conformations of the  $17\alpha$  side chain of **1** and **2** were also investigated by measuring NOE intensities between the vinyl protons and the aliphatic  $^1\text{H}$  of the C and D ring. The 2D NOESY of **1** and **2** reveal a similar pattern of NOE cross peaks and intensities between H20 and H21 with the aliphatic protons  $12\alpha$ ,  $12\beta$ , H14,  $15\alpha$ ,  $16\alpha$ , and  $16\beta$  (Figure 5). Selective 1D NOESY experiments of H20 and H21 allow a more detailed inspection of the NOE intensities (Figures 1(c) and 2(c), (d)). Table 6 and 7 summarize and compare the intensities of the observed NOE signals with expected NOE's based on H-H distances in all predicted low energy conformers of **1** and **2**.

The NOE data for **1** and **2** suggest a similarly preferred orientation of the  $17\alpha$  vinyl side chain. The absence of an observable NOE between H21 and  $12\alpha$  rules out conformers, **1c**, **2a**, **2b**, **2c**, **2g**, and **2h**, as contributing conformers, precluding most of the minima observed in the shallow energy surface range of  $85^\circ$  to  $165^\circ$  for dihedral C21-C20-C17-C13. The observable NOE's between H21 and H14,  $15\alpha$ , and  $16\alpha$  are consistent with **1b** and **2e**. The presence of the extended conformers, **1a**, **2d**, and **2f** are evident from the weak enhancements of  $15\alpha$  and  $16\alpha$  upon irradiation of H20.

## Conclusions

The NOE data of **1** and **2** and the statistical analysis of  $^{13}\text{C}$  chemical shifts are both

consistent with a preferred orientation of the  $17\alpha$  vinyl side chain. The findings from the multiple independent variable linear regression analyses of the  $^{13}\text{C}$  data of **1** and **2**, that conformers **1b** and **2e** are the major conformers, are compatible with the identity of the major conformers favored by NOE data. Conformer **1b** has the vinyl group turned under the D-ring, with the C-21 hydrogen projecting toward C15, and with the C-21 phenyl only slightly twisted out of the plane of the double bond. Conformer **2e** has the double bond disposed in a similar fashion, but has a greater torsion between the double bond and phenyl ring, that allows the ortho substituent to avoid A-strain and to project out from under the D-ring.

The statistical method and the NOE data do not agree on the identity of the minor conformers. For **1**, the regression analysis predicts a 12% population of the extended conformer **1a** that is consistent with the NOE data. However, the minor populations of **1c** and **2c** that appear in the statistical analyses are inconsistent with NOE data that instead favor **2d** and **2f** as minor conformers. The disagreements can be attributed to the limitation of the regression analysis due to the small  $^{13}\text{C}$  shift differences in the C and D ring among most of the MM3 predicted conformers. However, the ability of the regression analysis, based on predicted  $^{13}\text{C}$  shifts, to identify the same major conformer as identified by NOE data demonstrates that this approach to interpretation of chemical shift data is a useful complement to more common methods of conformational analysis.

This study reveals that the  $17\alpha$  substituents of **1** and **2** have a similar preferred orientation in reference to the steroidal skeleton. This similarity in solution conformations of **1** and **2** suggests that there are no inherent restrictions with respect to occupying a

similar receptor volume other than positional placement of the substituent. Other influences such as electronic effects may also play roles in the differing biological responses and RBA values of **1** and **2**. It is interesting to note the apparent absence of a similar range of conformational structures for the 20E-isomers **1** and **2** compared to the 20Z-isomers previously examined,<sup>3</sup> despite the predictions of favorable energies for other conformers in MM3 calculations. However, with only minor energy differences between conformers, this could be a case where the solution conformational preference could be overridden by interactions with the receptor.

### Acknowledgements

We thank Dr. Roger Kautz for valuable assistance concerning the NMR experiments. This work has been supported in part by PHS award R01-CA81 and a grant from the U.S. Army DAMD17-99-1-9333, and DAMD17-00-1-0384.

## References

1. Hanson RN, Lee CY, Friel C, DeSombre ER, Hughes A. *Steroids* (Submitted).
2. (a) Brzozowski AM, Pike AC, Dauter Z, Hubbard RE, Bonn T, Engstrom O, Ohman L, Greene GL, Gustafson JA. *Nature* 1997; **389**: 753; (b) Shiau AK, Barstad D, Loria PM, Cheng L, Kushner PJ, Agard DA, Greene GL. *Cell* 1998; **95**: 927.
3. Sebag AB, Friel CJ, Hanson RN, Forsyth DA. *J. Org. Chem.* 2000; **65**: 7902..
4. Forsyth DA, Sebag AB. *J. Am. Chem. Soc.* 1997; **119**: 9483.
5. Lee CY, Hanson RN. *Tetrahedron* 2000; **56**: 1623.
6. Bax A, Subramanian S. *J. Magn. Reson.* 1986; **65**: 565.
7. Shaka AJ, Barker PS, Freeman R. *J. Magn. Reson.* 1985; **64**: 547.
8. Bax A, Freeman R, Morris GA. *J. Magn. Reson.* 1981; **42**: 164.
9. Jeener J, Meier BH, Bachmann P, Ernst RR. *J. Chem. Phys.* 1979; **71**: 4546.
10. Kessler H, Oschkinat H, Griesenger C, Bermel W. *J. Magn. Reson.* 1986; **70**: 106.
11. (a) Allinger NL, Yuh YH, Lii JH. *J. Am. Chem. Soc.* 1989; **111**: 8551; (b) MM3(94) in Alchemy2000, Tripos, Inc.: St. Louis, MO.
12. (a) Gajewski JJ, Gilbert KE, McKelvie H. In *Advances in Molecular Modeling*; Liotta, D (ed.), JAI Press: Greenwich, CT, 1990; Vol. 2. (b) PCMODEL, V.6.0, Serena Software: Box 3076, Bloomington, IN.
13. Sebag AB, Forsyth DA, Plante MA. *J. Org. Chem.* (Submitted).
14. Gaussian 98, Revision A.3, Frisch MJ, Trucks GW, Schlegel HB, Scuseria GE, Robb MA, Cheeseman JR, Zakrzewski VG, Montgomery, Jr. JA, Stratmann RE, Burant JC,

Dapprich S, Millam JM, Daniels AD, Kudin KN, Strain MC, Farkas O, Tomasi J, Barone V, Cossi M, Cammi R, Mennucci B, Pomelli C, Adamo C, Clifford S, Ochterski J, Petersson GA, Ayala PY, Cui Q, Morokuma K, Malick DK, Rabuck AD, Raghavachari K, Foresman JB, Cioslowski J, Ortiz JV, Stefanov BB, Liu G, Liashenko A, Piskorz P, Komaromi I, Gomperts R, Martin RL, Fox DJ, Keith T, Al-Laham MA, Peng CY, Nanayakkara A, Gonzalez C, Challacombe M, Gill PMW, Johnson B, Chen W., Wong MW, Andres JL, Gonzalez C, Head-Gordon M, Replogle ES, Pople JA, Gaussian, Inc., Pittsburgh PA, 1998.

15. SPSS Base 10.0, SPSS Inc.: Chicago, IL, 1999.

16. Mooney CZ, Duval RD. *Bootstrapping*, Sage Publications, Inc.: Newbury Park, CA, 1993.

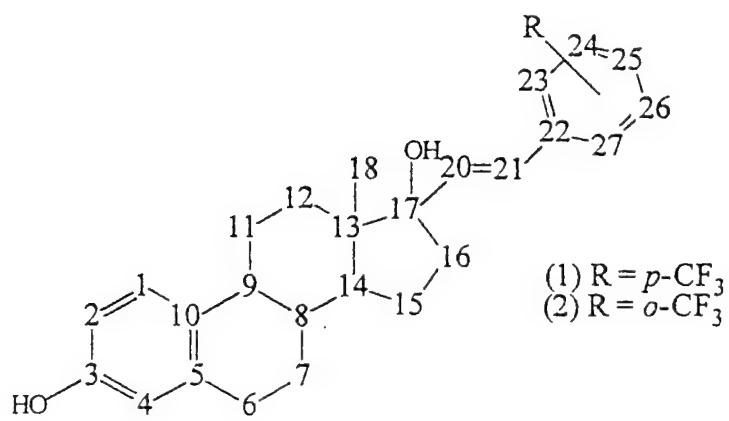


## Figure Captions

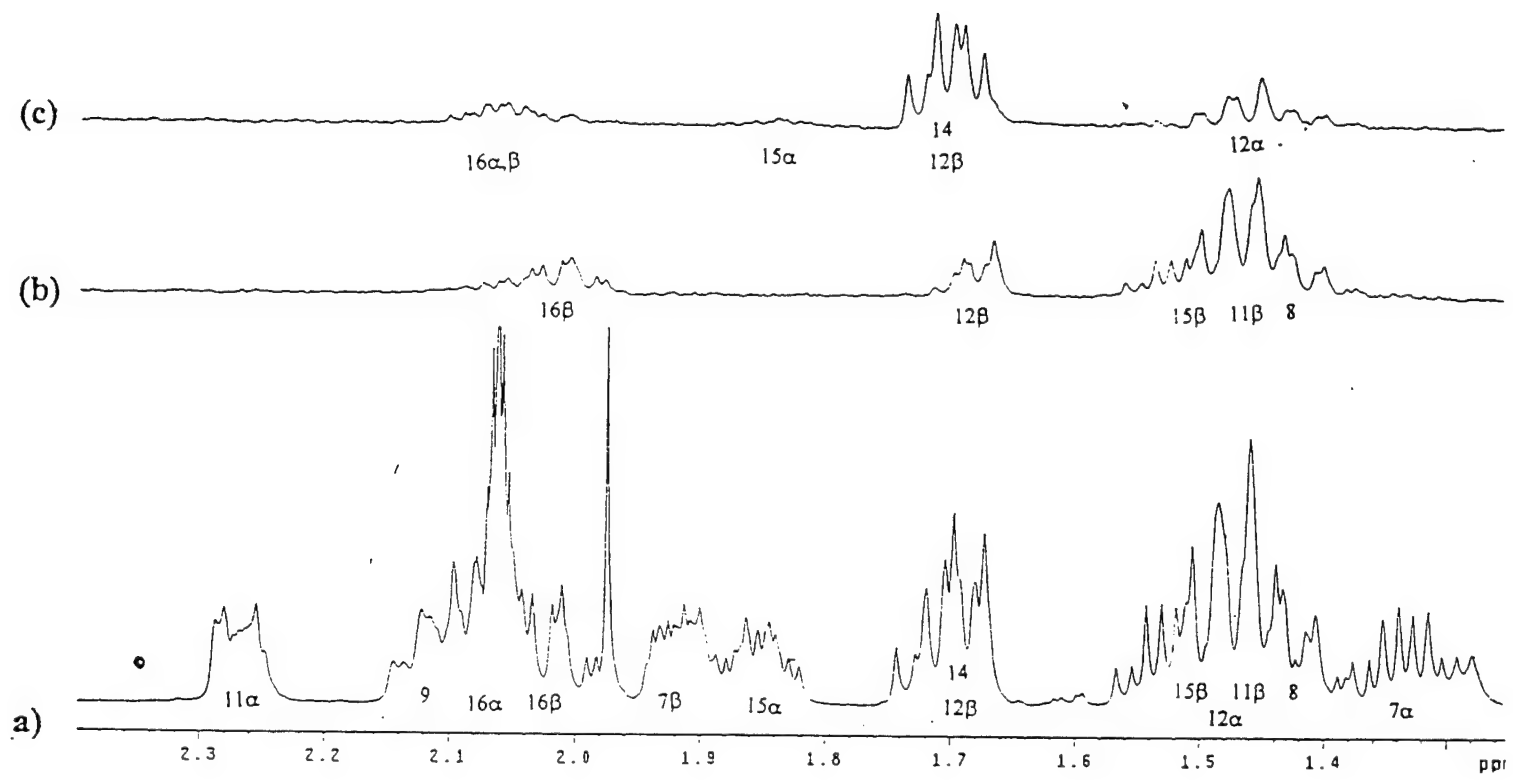
**Figure 1.** (a) Low frequency spectral region of the 500 MHz  $^1\text{H}$  NMR spectra of **1** in acetone- $d_6$ . Equivalent spectral regions of the 500 MHz 1D NOESY spectra (500 ms mixing time) of **1** obtained by selective irradiation of the C18 methyl (b), and H20/H21 (c) using a Gaussian pulse. Spectra (b) and (c) are 4x the vertical scale of (a). Overlap of H20 and H21 inhibited selective irradiation of each proton.

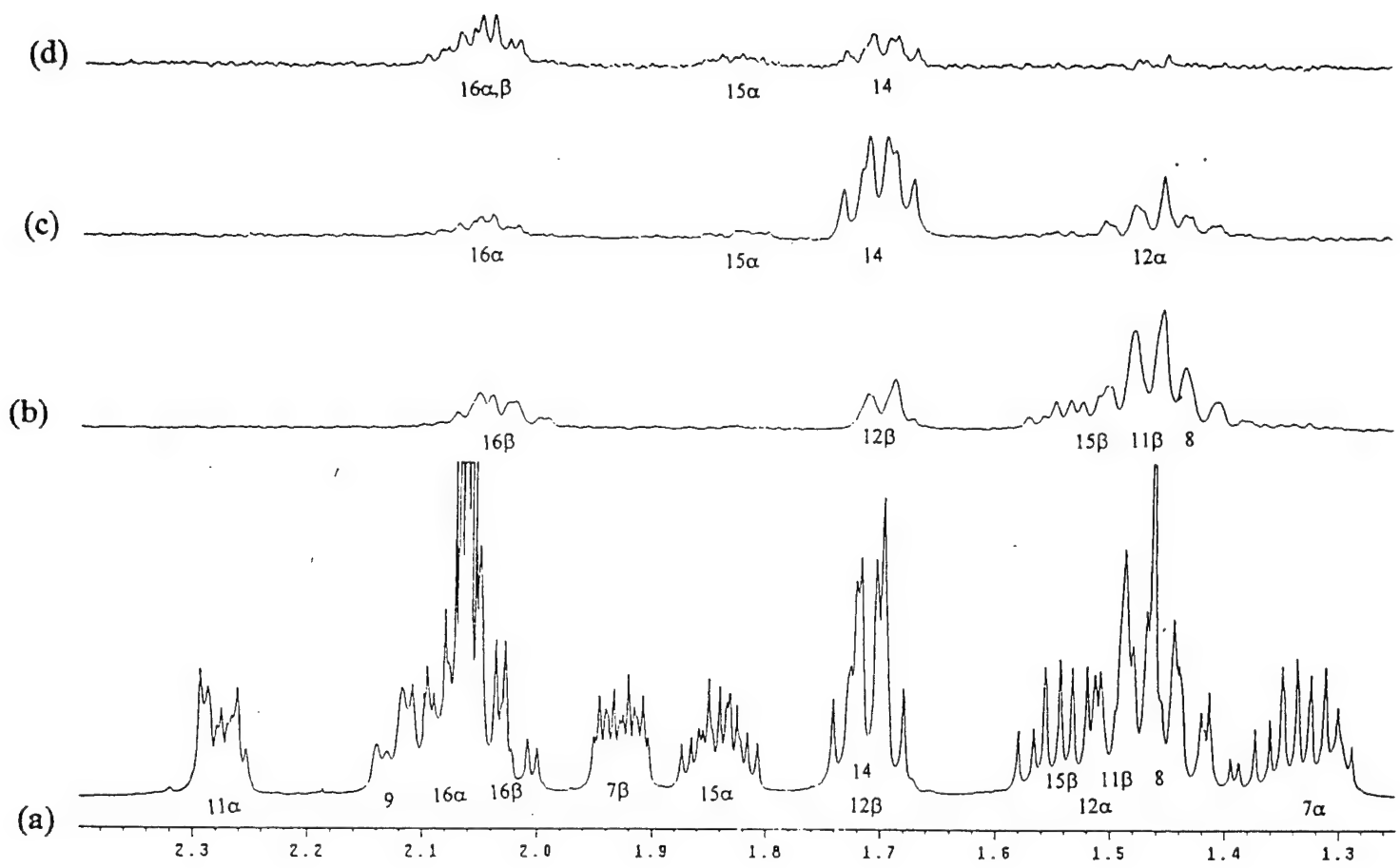
**Figure 2.** (a) Low frequency spectral region of the 500 MHz  $^1\text{H}$  NMR spectra of **2** in acetone- $d_6$ . Equivalent spectral regions of the 500 MHz 1D NOESY spectra (500 ms mixing time) of **2** obtained by selective irradiation of the C18 methyl (b), H20 (c), and H21 (d) using a Gaussian pulse. Spectra (b), (c), and (d) are 4x the vertical scale of (a).

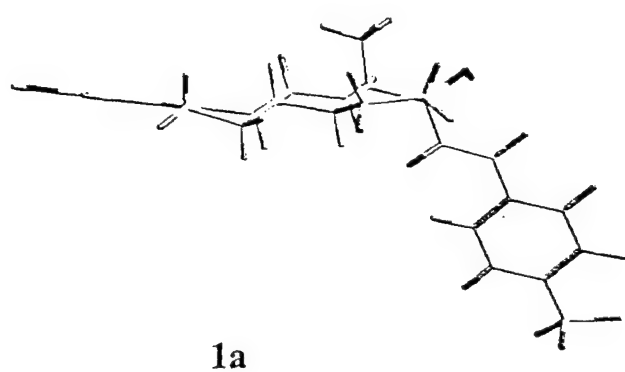
**Figure 3.** MM3-predicted geometries for the most stable conformers of **1**.

**Figure 4.** MM3-predicted geometries for the most stable conformers of **2**.

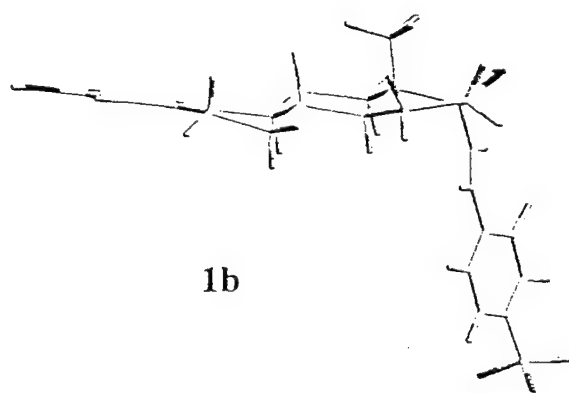
**Figure 5.** Spectral regions of the 500 MHz 2D NOESY spectrum of (a) **1** and (b) **2** obtained with a mixing time of 500 ms. The NOE connectivities are indicated.



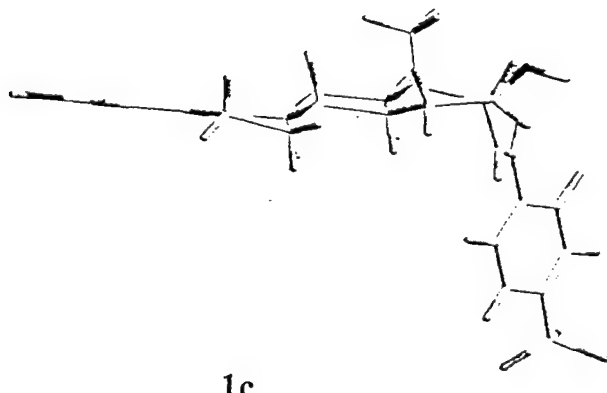




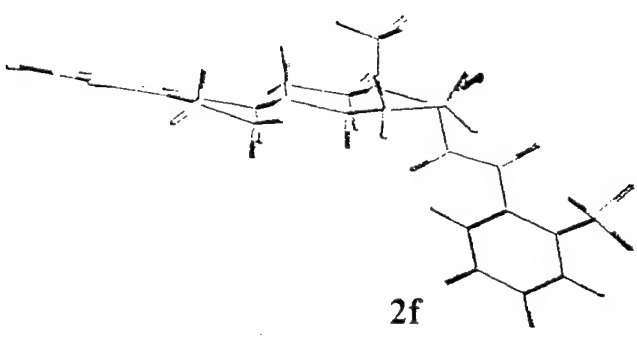
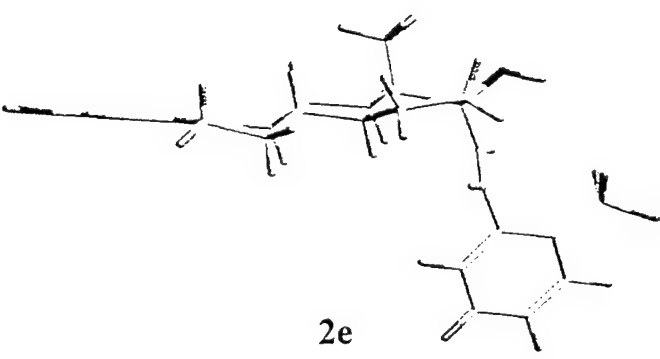
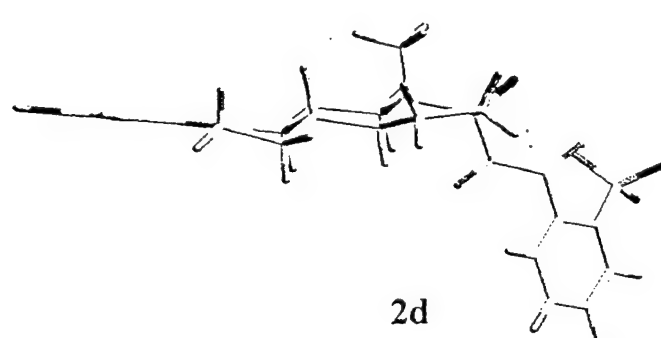
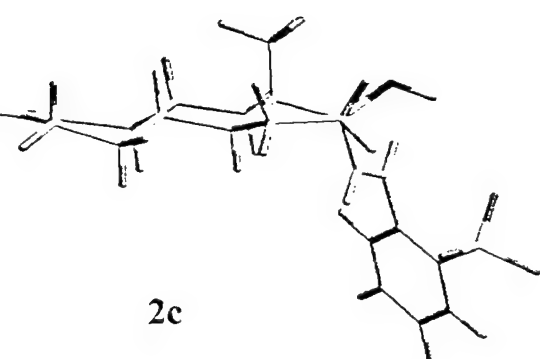
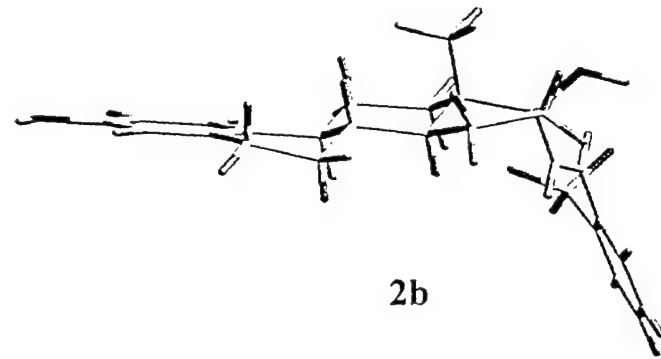
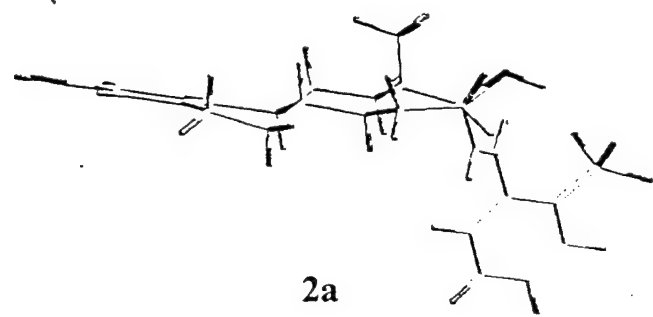
1a

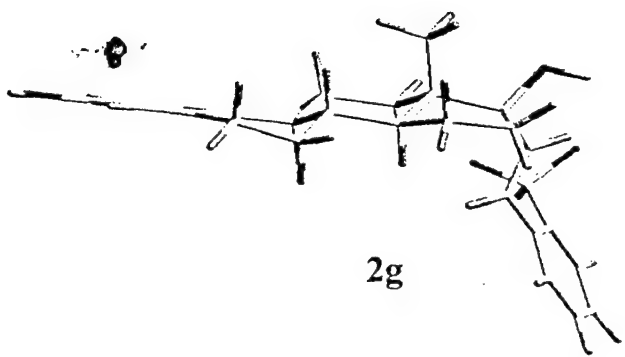


1b

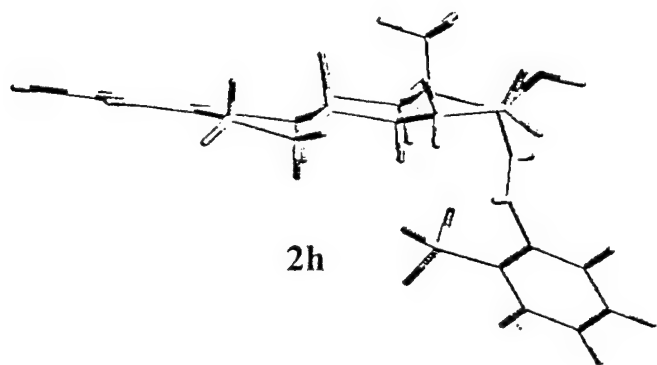


1c





2g



2h

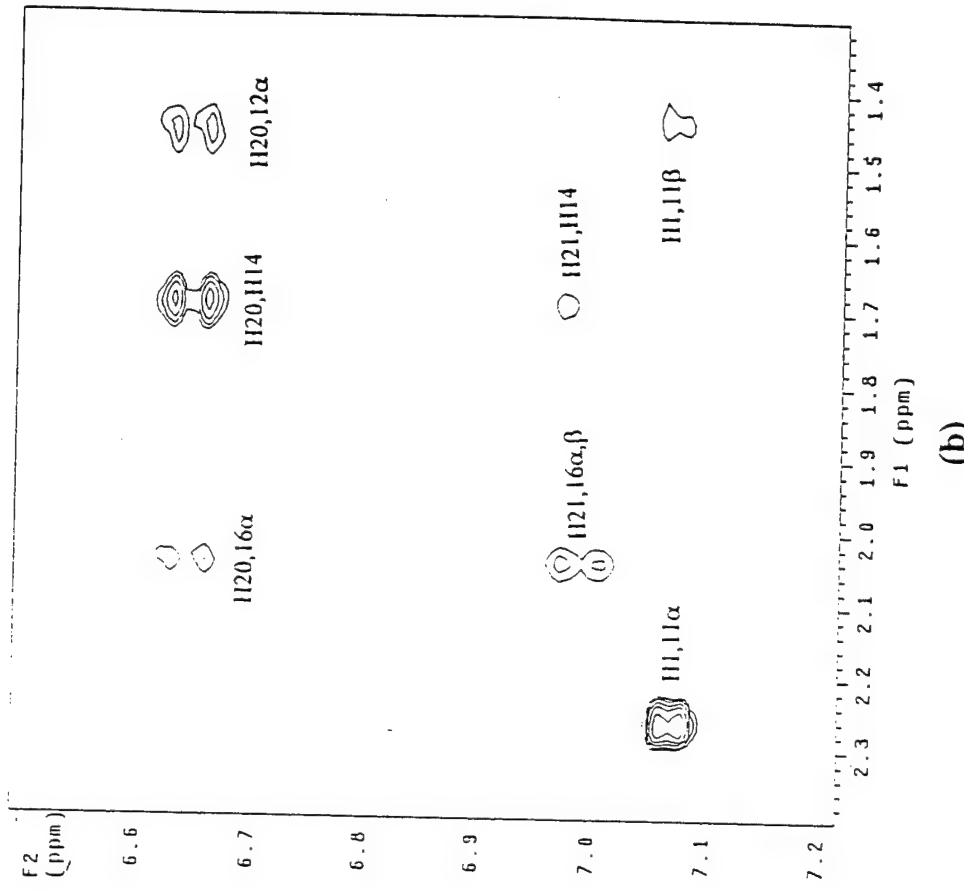
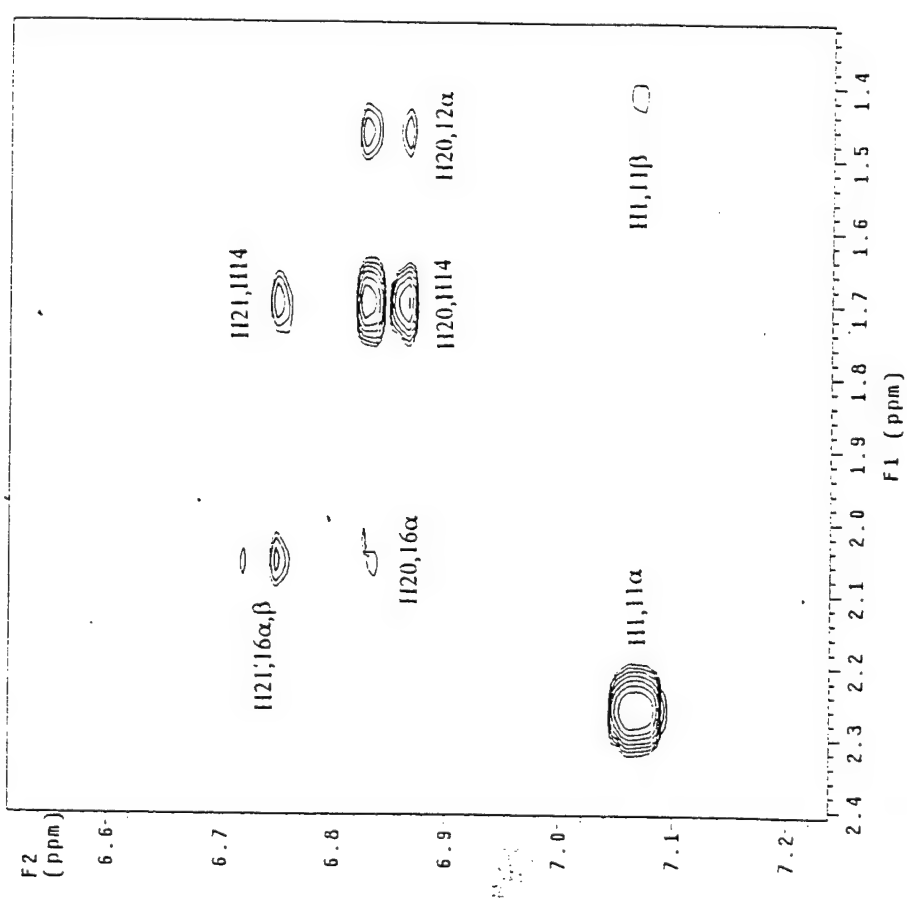


**Table 1.**  $^1\text{H}$  and  $^{13}\text{C}$  Chemical Shifts for **1** and **2**

$^1\text{H}$	<b>1</b>	<b>2</b>	$^{13}\text{C}$	<b>1</b>	<b>2</b>
1	7.09	7.09	1	126.4	126.4
2	6.58	6.59	2	112.9	112.9
4	6.52	6.54	3	155.3	155.2
6 $\alpha$	2.75	2.78	4	115.3	115.3
6 $\beta$	2.80	2.81	5	137.7	137.5
7 $\alpha$	1.32	1.34	6	30.0	29.9
7 $\beta$	1.92	1.92	7	27.7	27.7
8	1.43	1.54	8	40.1	40.0
9	2.10	2.10	9	44.0	44.0
11 $\alpha$	2.26	2.28	10	131.3	131.3
11 $\beta$	1.46	1.43	11	26.7	26.6
12 $\alpha$	1.42	1.50	12	32.9	32.8
12 $\beta$	1.68	1.69	13	47.8	47.8
14	1.70	1.71	14	49.5	49.4
15 $\alpha$	1.86	1.84	15	23.5	23.5
15 $\beta$	1.52	1.50	16	37.0	36.9
16 $\alpha$	2.04	2.04	17	83.6	83.7
16 $\beta$	2.06	2.06	18	14.2	14.1
CH <sub>3</sub>	1.02	1.01	20	140.0	141.8
20	6.74	6.65	21	125.3	122.9
21	6.85	7.0	22	142.1	137.8
23	7.69	N/A	23	127.0	127.6
24	7.64	7.70	24	125.6	125.7
25	N/A	7.61	25	128.9	132.6
26	7.64	7.44	26	125.6	127.2
27	7.69	7.82	27	128.2	128.0
N/A	N/A	N/A	CF <sub>3</sub>	125.4	125.7

**Table 2.** Relative Energies and Key Dihedrals of Predicted Conformers of **1** and **2** Using MM3

Conformers	C13-C17-C20-C21	C20-21-22-23	Relative Energies (kcal/mol)
<b>1a</b>	161	-169	0
<b>1b</b>	-96	18	0.30
<b>1c</b>	89	158	0.32
<b>2a</b>	87	-145	0
<b>2b</b>	95	151	0.06
<b>2c</b>	89	-56	0.92
<b>2d</b>	149	144	1.25
<b>2e</b>	-99	55	1.26
<b>2f</b>	162	-148	1.33
<b>2g</b>	-65	-49	1.53
<b>2h</b>	-95	-68	1.59

**Table 3.** Experimental and Predicted  $^{13}\text{C}$  Chemical Shifts (ppm) of Predicted Conformers of **1** Using B3LYP/3-21G(X,6-31+G\*)//MM3 Calculations

<b>Carbon</b>	<b>1a</b>	<b>1b</b>	<b>1c</b>	<b>expt</b>
C1	127.6	127.2	127.3	126.4
C2	113.2	113.1	113.1	112.9
C3	153.3	153.1	153.0	155.3
C4	116.1	115.8	115.7	115.3
C5	136.4	136.0	135.9	137.7
C6	31.2	30.8	30.7	30.0
C7	28.2	28.3	28.3	27.7
C8	40.3	39.8	39.5	40.1
C9	44.2	43.9	43.9	44.0
C10	131.6	131.5	131.8	131.3
C11	28.3	28.1	28.2	26.7
C12	31.4	31.8	32.4	32.9
C13	46.5	48.1	48.1	47.8
C14	50.2	48.0	47.9	49.5
C15	25.7	26.2	26.4	23.5
C16	45.9	36.8	39.2	37.0
C17	83.0	84.9	84.1	83.6
C18	15.2	16.6	15.5	14.2
C20	149.2	144.9	143.4	140.0
C21	133.9	131.6	131.3	125.3
C22	137.9	138.6	137.6	142.1
C23	121.6	122.4	122.0	127.0
C24	127.5	127.6	127.5	125.6
C25	132.2	131.7	131.8	128.9
C26	128.0	127.8	127.8	125.6
C27	129.3	128.5	129.2	128.2
C28	130.8	130.9	130.8	125.4

**Table 4.** Experimental and Predicted  $^{13}\text{C}$  Chemical Shifts (ppm) of Predicted Conformers of **2** Using B3LYP/3-21G(X,6-31+G\*)//MM3 Calculations

Carbon	2a	2b	2c	2d	2e	2f	2g	2h	expt
C1	127.4	127.6	127.3	127.5	127.5	127.4	127.6	127.6	126.4
C2	113.1	113.1	113.0	113.1	113.1	113.1	113.1	113.0	112.9
C3	153.1	152.9	153.0	153.0	153.0	153.1	153.1	152.9	155.2
C4	115.8	115.5	115.8	115.8	115.7	115.9	115.8	115.7	115.3
C5	136.2	135.8	136.1	136.1	136.1	136.3	136.2	136.2	137.5
C6	31.1	30.8	30.7	31.1	31.1	30.9	31.1	31.1	29.9
C7	28.3	28.4	28.1	28.3	28.3	28.2	28.4	28.3	27.7
C8	39.9	39.7	40.1	39.9	39.5	40.1	40.3	40.0	40.0
C9	44.3	44.4	44.2	44.3	44.3	44.3	44.5	44.2	44.0
C10	131.6	132.1	131.6	131.6	132.0	131.5	131.7	132.1	131.3
C11	28.3	28.5	28.5	28.2	28.3	28.2	28.4	28.4	26.6
C12	33.0	33.8	33.1	31.9	32.2	31.9	29.4	30.5	32.8
C13	48.1	48.6	48.0	47.7	47.2	47.2	48.6	47.6	47.8
C14	51.5	51.1	50.9	49.6	48.3	49.7	50.8	47.6	49.4
C15	26.0	26.5	26.0	25.8	26.4	25.6	26.8	26.1	23.5
C16	39.6	42.4	39.2	39.6	38.9	41.6	39.7	37.6	36.9
C17	83.6	83.9	84.6	84.0	83.6	84.0	81.9	85.5	83.7
C18	16.3	15.0	16.1	16.3	15.2	16.3	18.3	16.9	14.1
C20	146.2	146.7	151.2	146.3	151.1	147.5	149.6	151.2	141.8
C21	130.7	133.3	130.1	129.9	225.7	132.5	128.7	131.7	122.9
C22	137.2	137.5	140.8	138.6	140.4	138.7	140.7	140.6	137.8
C23	126.8	126.4	128.1	127.3	128.4	126.6	128.7	129.0	127.6
C24	131.9	131.9	130.7	132.1	130.9	131.9	130.9	131.0	125.7
C25	130.6	130.6	130.9	130.9	131.0	130.7	130.9	130.8	132.6
C26	127.8	127.6	129.5	127.7	129.5	127.7	129.3	129.0	127.2
C27	130.5	130.1	131.4	130.1	131.2	130.0	131.0	130.5	128.0
C28	126.8	126.5	126.0	126.3	126.2	126.6	126.3	126.1	125.7

**Table 5.** Summary of the Multiple Independent Variable Regression Analysis<sup>a</sup> of the Calculated <sup>13</sup>C Shifts of Predicted Conformers of **1** and **2**

Conformer	Estimate (%)	Standard Error (%)
<b>1a</b>	13	29
<b>1b</b>	72	32
<b>1c</b>	15	28
<b>2a</b>	0	14
<b>2b</b>	0	13
<b>2c</b>	33	18
<b>2d</b>	0	18
<b>2e</b>	65	33
<b>2f</b>	0	30
<b>2g</b>	0	4
<b>2h</b>	2	22

<sup>a</sup> Constraints: Each conformer is greater than or equal to 0 %. Each of the conformer sets **1a-1c** and **2a-2h** total to 100 %.

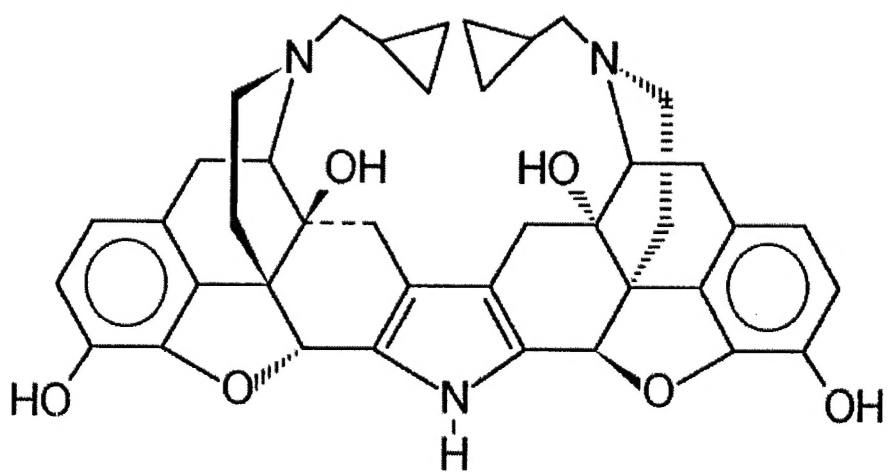
**Table 6.** Summary and Comparison of Observed NOE Enhancements with Expected NOE Intensities<sup>a</sup> for Predicted Conformers of **1**

<b>Irradiated</b>	<b>Enhanced</b>	<b>1a</b>	<b>1b</b>	<b>1c</b>	<b>Expt</b>
H20	12 $\alpha$	s	s	w	s
H20	H14	s	s	s	s
H20	15 $\alpha$	w	n	w	w
H20	16 $\alpha,\beta$	w	n	w	w
H21	12 $\alpha$	n	n	s	n
H21	H14,12 $\beta$	n	s	w	w
H21	15 $\alpha$	n	w	n	w
H21	16 $\alpha,\beta$	n	s	n	s

a. Expectations of strong (s), weak (w), and no (n) NOE enhancements correspond to H-H distances of 0 - 2.99; 3.0 - 4.99; and > 5 Å.

---

*The Philip S. Portoghesi  
Symposium in  
Medicinal Chemistry*



*August 23-24, 2001  
2-530 Moos Tower  
University of Minnesota*

Philip S. Portoghesi, Ph.D., is a University Distinguished Professor of Medicinal Chemistry at the University of Minnesota. A graduate of the University of Wisconsin Medicinal Chemistry department, he has served on the faculty at Minnesota since 1961. Dr. Portoghesi is a member of the editorial or editorial advisory boards of many journals and scientific organizations, and has been the Editor-in-Chief of the *Journal of Medicinal Chemistry* since 1972. He has received honorary doctorate degrees from the University of Catania, Italy and the Royal Danish School of Pharmacy. He is the recipient of many awards including the A.Ph.A. Research Achievement Award (1980), the Volwiler Award (1984), the ACS Medicinal Chemistry Award (1990), the AAPS Research Achievement Award in Medicinal Chemistry (1990), the Nathan Eddy Award (1991), the ACS Edward Smissman Award (1991), the Rho Chi Pharmacy Honor Society Award (1999), the Italian Chemical Society Oak & Tulip Award (1999), and the ACS Alfred Burger Award (2000). He is a fellow of the Academy of Pharmaceutical Sciences (1974), AAAS (1986), AAPS (1986) and College on Problems of Drug Dependence (1990).

Prof. Portoghesi has presented numerous lectures at national and international conferences, universities and industry, has authored over 315 publications and has trained approximately 95 students and postdoctoral research associates. His research interests are in the area of drug design with specific contributions to the area of opioid chemistry. The impact of his work on the field of drug design and receptor-ligand interactions is exemplified by him being listed as one of the most cited authors in the area of xenobiotics for the period 1981-1992.

On the occasion of his 70<sup>th</sup> birthday, we would like to celebrate Phil's outstanding contributions not only as a preeminent scholar in medicinal chemistry, but also in his teaching and mentoring of scientists, as well as his outstanding service as Editor of the *Journal of Medicinal Chemistry*. He has uniquely contributed to the quality and reputation of the Department of Medicinal Chemistry, the College of Pharmacy, and the University of Minnesota.

*work*  
MODERATOR: Rick Wagner, Ph.D., University of Minnesota

*Good talk*

1:30 "DESIGN AND SYNTHESIS OF PEPTIDASE  
INHIBITORS. WHAT CHALLENGES REMAIN?" *movement of protein*

*work* 1:30 Daniel H. Rich, Ph.D., University of Wisconsin *x-ray*  
peptidase design

2:10 "DESIGN, SYNTHESIS AND EVALUATION OF NOVEL  
STEROIDAL ANTIESTROGENS FOR THE TREATMENT OF  
HORMONE RESPONSIVE BREAST CANCER" *55%*

*work* 2:10 Robert N. Hanson, Ph.D., Northeastern University

2:50-3:20 Break

3:20 "G-QUADRUPLEXES AND ASSOCIATED GENE TARGETS  
FOR DRUG DESIGN" *57.4%* *~50 min*

*work* 3:20 Laurence H. Hurley, Ph.D., University of Arizona

3:40 "BENZODIAZEPINE CCK-A RECEPTOR AGONISTS" *Good talk*

*work* 3:40 Elizabeth E. Sugg, Ph.D., GlaxoSmithKline Company

4:20 "2(3H)-BENZOTIAZOLONES, AN INEXHAUSTIBLE  
SOURCE OF INSPIRATION FOR AN ACADEMIC  
MEDICINAL CHEMIST. APPLICATION TO THE DESIGN  
OF MIXED AFFINITY LIGANDS FOR 5-HT SUB-CLASSES"

*work* 4:20 Jacques Poupaert, Ph.D., University of Louvan, Belgium *looks like Keenan Wayne*

6:30 Reception - Cash Bar  
McNamara Alumni Center, A.I. Johnson Great Room

7:30 Dinner - Pre-registered guests only  
McNamara Alumni Center, A.I. Johnson Great Room

---

MODERATOR: Herbert Nagasawa, Ph.D., *University of Minnesota*

1:30    ***"OPIOID RESEARCH TOOLS AND DRUGS FOR THE  
NEW MILLENNIUM"***

Kenner C. Rice, Ph.D., *National Institutes of Health*

2:10    ***"DESIGN AND SYNTHESIS OF NOVEL PEPTIDE-BASED  
AFFINITY LABELS FOR OPIOID RECEPTORS"***

Jane V. Aldrich, Ph.D., *University of Maryland*

2:50-3:20      Break

3:20    ***"DEVELOPMENT OF POTENT AND HIGHLY SELECTIVE  
SMALL MOLECULE INHIBITORS OF VLA4"***

Francine S. Grant, Ph.D., *Elan Pharmaceuticals*

4:00    ***"SELECTIVE MECHANISM-BASED INHIBITION OF THE  
QUINONE-DEPENDENT AMINE OXIDASES"***

Lawrence M. Sayre, Ph.D., *Case Western Reserve University*

4:40    Symposium Summation

Yusuf Abul-Hajj, Ph.D.

4:45    ***"WORDS OF WISDOM"***

Philip S. Portoghesi, Ph.D.